

Forecasting range shifts of a dioecious plant species under climate change

Jacob K. Moutouama 0000-0003-1599-1671^{*1}, Aldo Compagnoni 0000-0001-8302-7492², and Tom E.X. Miller 0000-0003-3208-6067¹

¹Program in Ecology and Evolutionary Biology, Department of BioSciences, Rice University, Houston, Texas, USA

²Institute

of Biology, Martin Luther University Halle-Wittenberg, Halle, Germany; and German Centre for Integrative Biodiversity Research (iDiv), Leipzig, Germany

Running header: Forecasting range shifts

Keywords: demography, forecasting, global warming, matrix projection model, population dynamics, sex ratio, range limits

Submitted to: *Ecology letters* (Letter)

Data accessibility statement: All data used in this paper are publicly available and cited appropriately (Miller and Compagnoni, 2022a). Should the paper be accepted, all computer scripts supporting the results will be archived in a Zenodo package, with the DOI included at the end of the article. During peer review, our code (Stan and R) is available at <https://github.com/jmoutouama/POAR-Forecasting>.

Conflict of interest statement: None.

Authorship statement: J.K.M., A.C. and T.E.X.M. designed the study. A.C. and T.E.X.M. collected the data. All authors conducted the statistical analyses and modeling. J.K.M. drafted the manuscript, and T.E.X.M contributed to revisions.

Abstract:

Main Text:

Figures: 6

Tables: 0

References: 106

*Corresponding author: jmoutouama@gmail.com

¹ Abstract

² Global climate change has triggered an urgent need for predicting the reorganization of Earth's
³ biodiversity. Currently, the vast majority of models used to forecast population viability and
⁴ range shifts in response to climate change ignore the complication of sex structure, and thus
⁵ the potential for females and males to differ in their sensitivity to climate drivers. We developed
⁶ demographic models of range limitation, parameterized from geographically distributed com-
⁷ mon garden experiments, with females and males of a dioecious grass species (*Poa arachnifera*)
⁸ throughout and beyond its range in the south-central U.S. Female-dominant and two-sex
⁹ model versions both predict that future climate change will alter population viability and
¹⁰ will induce a poleward niche shift beyond current northern limits. However, the magnitude of
¹¹ niche shift was underestimated by the female-dominant model, because females have broader
¹² temperature tolerance than males and become mate-limited under female-biased sex ratios.
¹³ Our result illustrate how explicit accounting for both sexes could enhance population viability
¹⁴ forecasts and conservation planning for dioecious species in response to climate change.

15 **Introduction**

16 Rising temperatures and extreme drought events associated with global climate change are
17 leading to increased concern about how species will become redistributed across the globe
18 under future climate conditions (Bertrand et al., 2011; Gamelon et al., 2017; Smith et al., 2024).
19 Species' range limits, when not driven by dispersal limitation, should generally reflect the limits
20 of the ecological niche (Lee-Yaw et al., 2016). Niches and geographic ranges are often limited
21 by climatic factors including temperature and precipitation (Sexton et al., 2009). Therefore,
22 any substantial changes in the magnitude of these climatic factors could impact population
23 viability, with implications for range expansions or contractions based on which regions of
24 a species' range become more or less suitable (Davis and Shaw, 2001; Pease et al., 1989).

25 Forecasting range shifts for dioecious species (most animals and ca. 7% of plant species)
26 is complicated by the potential for sexual niche differentiation, i.e. distinct responses of
27 females and males to shared climate drivers (Hultine et al., 2016; Morrison et al., 2016; Pottier
28 et al., 2021; Tognetti, 2012). The lower cost of reproduction for one sex (male or female)
29 may allow that sex to invest its energy in other functions that produce higher growth rates,
30 greater clonality, or even higher survival rates compared to the other sex, leading to sexual
31 niche differentiation (Bruijning et al., 2017). Accounting for sexual niche differentiation
32 is a long-standing challenge in accurately predicting which sex will successfully track
33 environmental change and how this will impact population viability and range shifts (Gissi
34 et al., 2023; Jones et al., 1999). Populations in which males are rare under current climatic
35 conditions could experience low reproductive success due to sperm or pollen limitation that
36 may lead to population decline in response to climate change that disproportionately favors
37 females (Eberhart-Phillips et al., 2017). In contrast, climate change could expand male habitat
38 suitability (e.g. upslope movement), which might increase seed set for mate-limited females
39 and favor range expansion (Petry et al., 2016). Across dioecious plants, for example, studies
40 suggest that future climate change toward hotter and drier conditions may favor male-biased
41 sex ratios (Field et al., 2013; Hultine et al., 2016). Although the response of species to climate
42 warming is an urgent and active area of research, few studies have disentangled the interaction
43 between sex and climate drivers to understand their combined effects on population dynamics
44 and range shifts, despite calls for such an approach (Gissi et al., 2023; Hultine et al., 2016).

45 The vast majority of theory and models in population biology, including those used
46 to forecast biodiversity responses to climate change, ignore the complication of sex structure
47 (but see Ellis et al., 2017; Gissi et al., 2024; Pottier et al., 2021). Traditional approaches instead
48 focus exclusively on females, assuming that males are in sufficient supply as to never limit
49 female fertility. In contrast, "two-sex" models are required to fully account for demographic

50 differences between females and males and sex-specific responses to shared climate drivers
51 (Gerber and White, 2014; Miller et al., 2011). Sex differences in maturation, reproduction,
52 and mortality schedules can generate skew in the operational sex ratio (OSR; sex ratio of
53 individuals available for mating) even if the birth sex ratio is 1:1 (Eberhart-Phillips et al., 2017;
54 Shelton, 2010). Climate and other environmental drivers can therefore influence the OSR
55 via their influence on sex-specific demographic rates. In a two-sex framework, demographic
56 rates both influence and respond to the OSR in a feedback loop that makes two-sex models
57 inherently nonlinear and more data-hungry than corresponding female-dominant models.
58 Given the additional complexity and data needs, forecasts of range dynamics for dioecious
59 species under future climate change that explicitly account for females, males, and their
60 inter-dependence are limited (Lynch et al., 2014; Petry et al., 2016).

61 Tracking the impact of climate change on population viability (λ) and distributional
62 limits of dioecious taxa depends on our ability to build mechanistic models that take into
63 account the spatial and temporal context of sex specific response to climate change, while
64 accounting for sources of uncertainty (Davis and Shaw, 2001; Evans et al., 2016). Structured
65 population models built from demographic data collected from geographically distributed
66 observations or common garden experiments provide several advantages for studying
67 the impact of climate change on species' range shifts (Merow et al., 2017; Schultz et al.,
68 2022; Schwinning et al., 2022). First, demographic models link individual-level life history
69 events (mortality, development, and regeneration) to population demography, allowing the
70 investigation of factors explaining vital rate responses to environmental drivers (Dahlgren
71 et al., 2016; Ehrlén and Morris, 2015; Louthan et al., 2022). Second, demographic models
72 have a natural interface with statistical estimation of individual-level vital rates that provide
73 quantitative measures of uncertainty and isolate different sources of variation, features that
74 can be propagated to population-level predictions (Elderd and Miller, 2016; Ellner et al.,
75 2022). Finally, structured demographic models can be used to identify which aspects of
76 climate are the most important drivers of population dynamics. For example, Life Table
77 Response Experiments (LTRE) built from structured models have become widely used to
78 understand the relative importance of covariates in explaining variation in population growth
79 rate (Czachura and Miller, 2020; Ellner et al., 2016; Hernández et al., 2023).

80 In this study, we combined geographically-distributed common garden experiments,
81 hierarchical Bayesian statistical modeling, two-sex population projection modeling, and climate
82 back-casting and forecasting to understand demographic responses to climate change and their
83 implications for past, present, and future range dynamics. Our work focused on the dioecious
84 plant Texas bluegrass (*Poa arachnifera*), which is distributed along environmental gradients
85 in the south-central U.S. corresponding to variation in temperature across latitude and

86 precipitation across longitude (Fig. 1A)¹. This region has experienced rapid climate warming
87 since 1900 and this is projected to continue through the end of the century (Fig. 1 B and C). Our
88 previous study showed that, despite evidence for differentiation of climatic niche between sexes,
89 the female niche mattered the most in driving longitudinal range limits of Texas bluegrass
90 (Miller and Compagnoni, 2022b). However, that study used a single proxy variable (longitude)
91 to represent environmental variation related to aridity and did not consider variation in
92 temperature, which is the much stronger dimension of forecasted climate change in this region
93 (Fig. S-2). Developing a rigorous forecast for the implications of future climate change requires
94 that we transition from implicit to explicit treatment of multiple climate drivers, as we do
95 here. Leveraging the power of Bayesian inference, we take a probabilistic view of past, present,
96 and future range limits by quantifying the probability of population viability ($Pr(\lambda \geq 1)$) in
97 relation to climate drivers of demography, an approach that fully accounts for uncertainty
98 arising from multiple sources of estimation and process error. Specifically, we asked:

- 99 1. What are the sex-specific vital rate responses to variation in temperature and precipitation
100 across the species' range?
- 101 2. How do sex-specific vital rates combine to determine the influence of climate variation
102 on population growth rate (λ)?
- 103 3. What is the impact of climate change on operational sex ratio throughout the range?
- 104 4. What are the likely historical and projected dynamics of the Texas bluegrass geographic
105 niche and how does accounting for sex structure modify these predictions?

106 Materials and methods

107 Study species and climate context

108 Texas bluegrass (*Poa arachnifera*) is a dioecious perennial, summer-dormant cool-season (C3)
109 grass that occurs in the south-central U.S. (Texas, Oklahoma, and southern Kansas) (Figure
110 1) (Hitchcock, 1971). Texas bluegrass grows between October and May, flowers in spring,
111 and goes dormant during the hot summer months of June to September (Kindiger, 2004).
112 Following this life history, we divided the calendar year into growing (October 1 - May
113 31) and dormant (June 1 - September 30) seasons in the analyses below. Biological sex is
114 genetically based and the birth (seed) sex ratio is 1:1 (Renganayaki et al., 2005). Females and
115 males are morphologically indistinguishable except for their inflorescences. Like all grasses,
116 this species is wind pollinated (Hitchcock, 1971) and most male-female pollen transfer occurs

¹Fig. A does not show what we are saying here. Maybe I should add the Figure with the raster

¹¹⁷ within 10-15m (Compagnoni et al., 2017). Surveys of 22 natural populations throughout the
¹¹⁸ species' distribution indicated that operational sex ratio (the female fraction of inflorescences)
¹¹⁹ ranged from 0.007 to 0.986 with a mean of 0.404 (Miller and Compagnoni, 2022b).

¹²⁰ Latitudinal limits of the Texas bluegrass distribution span 7.74 °C to 16.94 °C of
¹²¹ temperature during the dormant season and 24.38 °C to 28.80 °C during the dormant season.
¹²² Longitudinal limits span 244.9 mm to 901.5 mm of precipitation during the growing season
¹²³ and 156.3 mm to 373.3 mm. This region has experienced *ca.* 0.5 °C of climate warming since
¹²⁴ 1900, with faster warming during the cool-season months ($0.0055^{\circ}\text{C}/\text{yr}$) than the hot summers
¹²⁵ ($0.0046^{\circ}\text{C}/\text{yr}$) (Fig. S-1). Future warming is projected to accelerate to $0.03 - 0.06^{\circ}\text{C}/\text{yr}$ by
¹²⁶ the end of the century depending on the season and forecast model. On the other hand,
¹²⁷ precipitation has increased over the past century for much of the region but is forecasted
¹²⁸ to decline back to early-20th century levels (Fig. S-1). ²

¹²⁹ Common garden experiment

¹³⁰ Experimental design

¹³¹ We conducted a range-wide common garden experiment to quantify sex-specific demographic
¹³² responses to climate variation. Details of the experimental design are provided in Miller
¹³³ and Compagnoni (2022b); we provide a brief overview here. The experiment was installed
¹³⁴ at 14 sites throughout and, in some cases, beyond the natural range of Texas bluegrass that
¹³⁵ sampled a broad range of latitude and longitude (Figure 1A). At each site, we established
¹³⁶ 14 blocks. For each block we planted three female and three male individuals that were
¹³⁷ clonally propagated from females and males from eight natural source populations (Figure
¹³⁸ 1A); because sex is genetically-based, clones never deviated from their expected sex. The
¹³⁹ experiment was established in November 2013 with a total of 588 female and 588 male plants,
¹⁴⁰ and was censused in May of 2014, 2015, and 2016. At each census, we collected data on
¹⁴¹ survival, size (number of tillers), and number of panicles (reproductive inflorescences). For
¹⁴² the analyses that follow, we focus on the 2014-15 and 2015-16 transition years, since the start
¹⁴³ of the experiment did not include the full 2013-14 transition year.

²*I like this but I don't know if this not a repetition of what we've said in the introduction about climate change in the study area.*

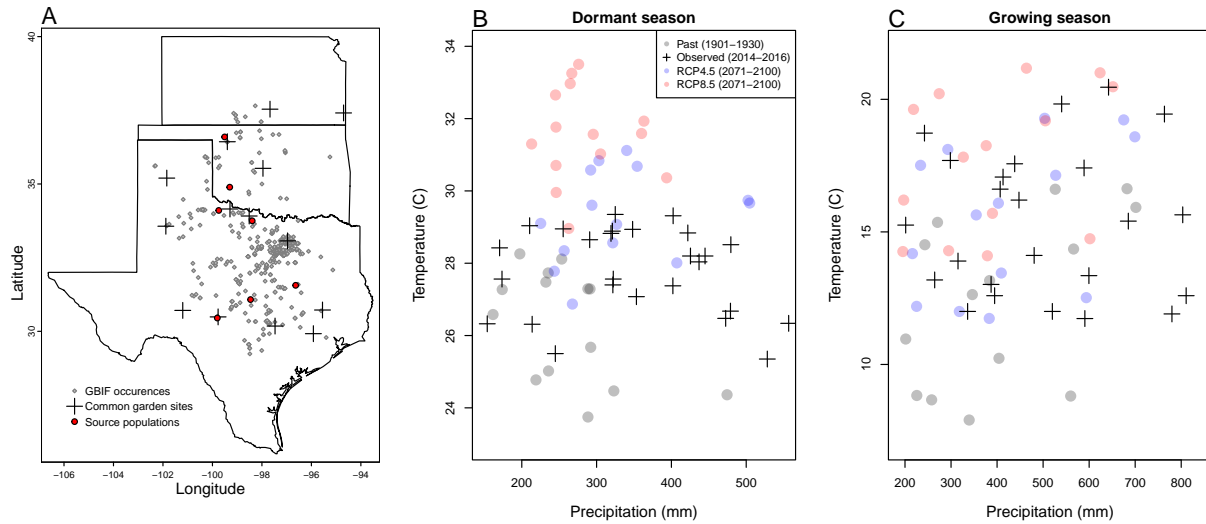


Figure 1: Experimental gardens and climate of the study region. **A:** Map of 14 experimental garden sites (crosses) in Texas, Oklahoma, and Kansas relative to GBIF occurrences of *Poa arachnifera* (gray points). Red points indicate source populations for plants used in the common garden experiment. **B,C:** Past, future, and observed climate space for growing and dormant seasons. Crosses show observed conditions for the sites and years of the common garden experiment. Gray points show historical (1901-1930) climate normals, and blue and red points show end-of-century (2071-2100) climate normals for RCP4.5 and RCP8.5 projections, respectively, from MIROC5. See also (Figure ?? for more information about historical and projected climate change in the study region.

144 Climatic data collection

145 We gathered downscaled monthly temperature and precipitation for each site from Chelsa
 146 (Karger et al., 2017) to describe observed climate conditions during our study period. These
 147 climate data were used as covariates in vital rate regressions. We aligned the climatic years
 148 to match demographic transition years (June 1 – May 31) and growing and dormant seasons
 149 within each year. To back-cast and forecast demographic responses to changes in climate
 150 throughout the study region, we also gathered projection data for three 30-year periods: “past”
 151 (1901-1930), “current” (1990-2019) and “future” (2070-2100). Data for future climatic periods
 152 were downloaded from four general circulation models (GCMs) selected from the Coupled
 153 Model Intercomparison Project Phase 5 (CMIP5): Model for Interdisciplinary Research on
 154 Climate (MIROC5), Australian Community Climate and Earth System Simulator (ACCESS1-3),
 155 Community Earth System Model (CESM1-BGC), Centro Euro-Mediterraneo sui Cambiamenti
 156 Climatici Climate Model (CMCC-CM). All the GCMs were also downloaded from Chelsa
 157 (Sanderson et al., 2015). We evaluated future climate projections from two scenarios of
 158 representative concentration pathways (RCPs): RCP4.5, an intermediate-to-pessimistic scenario
 159 assuming a radiative forcing amounting to 4.5 W m^{-2} by 2100, and RCP8.5, a pessimistic

¹⁶⁰ emission scenario which projects a radiative forcing of 8.5 Wm^{-2} by 2100 (Schwalm et al.,
¹⁶¹ 2020; Thomson et al., 2011).

¹⁶² Projection data for the three 30-year periods included warmer or colder conditions than ob-
¹⁶³ served in our experiment, so extending our inferences to these conditions required some extrap-
¹⁶⁴ olation. However, across all sites, both study years were 1-2°C warmer than their correspond-
¹⁶⁵ ing “current” (1990-2019) temperature normals (Fig. S-2). Additionally, the 2014–15 growing
¹⁶⁶ season was generally wetter and cooler across the study region than 2015–16 (Fig. S-2). Com-
¹⁶⁷ bined, the geographic and inter-annual replication of the common garden experiment provided
¹⁶⁸ good coverage of most past and future conditions throughout the study region (Fig. 1B,C).

¹⁶⁹ **Sex-specific demographic responses to climatic variation across common garden sites**

¹⁷⁰ We used individual-level measurements of survival, growth (change in number of tillers), flow-
¹⁷¹ ering, and number of panicles (conditional on flowering) to develop Bayesian mixed effect mod-
¹⁷² els describing how each vital rate varies as a function of sex, size, and four climate covariates
¹⁷³ (precipitation and temperature of growing and dormant season)(Supplementary Method S.2.1).
¹⁷⁴ These vital rate models included main effects of size (the natural log of tiller number), sex, and
¹⁷⁵ seasonal climate covariates. Climate variables were fit with second-degree polynomial func-
¹⁷⁶ tions to accommodate the possibility of hump-shaped relationships (reduced demographic per-
¹⁷⁷ formance at both extremes). We also included two-way interactions between sex and each cli-
¹⁷⁸ mate driver and between temperature and precipitation within each season, and a three-way in-
¹⁷⁹ teraction between sex, temperature, and precipitation within each season. We modeled survival
¹⁸⁰ and flowering data with a Bernoulli distribution and the growth (tiller number) with a zero-
¹⁸¹ truncated Poisson inverse Gaussian distribution. Fertility (panicle count conditional on flower-
¹⁸² ing) was modeled as zero-truncated negative binomial. We used generic, weakly informative
¹⁸³ priors to fit coefficients for survival, growth, flowering models ($\beta \sim N(0, 1.5)$) and random
¹⁸⁴ effect variances ($\sigma \sim \text{Gamma}(\gamma(0.1, 0.1))$). We fit fertility model with also weakly informative pri-
¹⁸⁵ ors for coefficients ($\beta \sim N(0, 0.15)$). Different priors were used for fertility because the panicle
¹⁸⁶ model has a large number of parameters relative to the amount of available data (subset of our
¹⁸⁷ data) and because these specifics priors help prevent the model from overfitting. Each vital rate
¹⁸⁸ also includes normally distributed random effects for block-to-block variation ($\phi \sim N(0, \sigma_{block})$),
¹⁸⁹ site to site variation ($\nu \sim N(0, \sigma_{site})$), and source-to-source variation that is related to the genetic
¹⁹⁰ provenance of the transplants used to establish the common garden ($\rho \sim N(0, \sigma_{source})$).

191 **Sex ratio responses to climatic variation across common garden sites**

192 We also used the experimental data to investigate how climatic variation across the range
193 influenced sex ratio and operational sex ratio of the common garden populations. To do so,
194 we developed two Bayesian linear models using data collected during three years. Each model
195 had OSR or SR as response variable and a climate variable (temperature and precipitation
196 of the growing season and dormant season) as predictor (Supplementary Method S.2.2). We
197 modeled the OSR or SR data with a Bernoulli distribution and used non informative priors
198 for each coefficient ($\omega \sim N(0, 100)$).

199 **Model-fitting procedures**

200 All models were fit using Stan (Stan Development Team, 2023) in R 4.3.1 (R Core Team,
201 2023). We centered and standardized all climatic predictors to mean zero, variance one, which
202 facilitated model convergence. We ran three chains for 1000 samples for warmup and 4000
203 for sampling, with a thinning rate of 3. We assessed the quality of the models using posterior
204 predictive checks (Piironen and Vehtari, 2017) (Figure S-3).

205 **Two-sex and female-dominant matrix projection models**

206 We used the climate-dependent vital rate regressions estimated above, combined with
207 additional data sources, to build female-dominant and two-sex versions of a climate-explicit
208 matrix projection model (MPMs) structured by the discrete state variables size (number
209 of tillers) and sex. The female-dominant and two-sex versions of the model both allow
210 for sex-specific response to climate and differ only in the feedback between operational
211 sex ratio and seed fertilization. For clarity of presentation we do not explicitly include
212 climate-dependence in the notation below, but the following model was evaluated over
213 variation in seasonal temperature and precipitation.

Let $F_{x,t}$ and $M_{x,t}$ be the number of female and male plants of size x in year t , where $x \in [1, \dots, U]$. The minimum possible size is one tiller and U is the 95th percentile of observed maximum size (35 tillers). Let F_t^R and M_t^R be new female and male recruits in year t , which we treat as distinct from the rest of the size distribution because we assume they do not reproduce in their first year, consistent with our observations. For a pre-breeding census,

the expected numbers of recruits in year $t+1$ is given by:

$$F_{t+1}^R = \sum_1^U [p^F(x) \cdot c^F(x) \cdot d \cdot v(\mathbf{F}_t, \mathbf{M}_t) \cdot m \cdot \rho] F_{x,t} \quad (1)$$

$$M_{t+1}^R = \sum_1^U [p^F(x) \cdot c^F(x) \cdot d \cdot v(\mathbf{F}_t, \mathbf{M}_t) \cdot m \cdot (1-\rho)] F_{x,t} \quad (2)$$

where p^F and c^F are flowering probability and panicle production for females of size x , d is the number of seeds per female panicle, v is the probability that a seed is fertilized, m is the probability that a fertilized seed germinates, and ρ is the primary sex ratio (proportion of recruits that are female), which we assume to be 0.5 (Miller and Compagnoni, 2022b).

In the two-sex model, seed fertilization is a function of population structure, allowing for feedback between vital rates and operational sex ratio (OSR). In the context of the model, OSR is defined as the fraction of panicles that are female and is derived from the $U \times 1$ vectors \mathbf{F}_t and \mathbf{M}_t :

$$v(\mathbf{F}_t, \mathbf{M}_t) = v_0 * \left[1 - \left(\frac{\sum_1^U p^F(x, z) c^F(x, z) F_{x,t}}{\sum_1^U p^F(x, z) c^F(x, z) F_{x,t} + p^M(x, z) c^M(x, z) M_{x,t}} \right)^\alpha \right] \quad (3)$$

The summations tally the total number of female and male panicles over the size distribution, giving the fraction of total panicles that are female. We focus on the female fraction of panicles and not female fraction of reproductive individuals because panicle number can vary widely depending on size; we assume that few males with many panicles vs. many males with few panicles are interchangeable pollination environments. Eq. 3 has the properties that seed fertilization is maximized at v_0 as OSR approaches 100% male, goes to zero as OSR approaches 100% female, and parameter α controls how female seed viability declines as male panicles become rare. We estimated these parameters using data from a sex ratio manipulation experiment, conducted in the center of the range, in which seed fertilization was measured in plots of varying OSR; this experiment is described elsewhere (Compagnoni et al., 2017) and is summarized in [Supplementary Method S.2.3](#)³. This experiment also provided estimates for seed number per panicle (d) and germination rate (m). Lacking data on climate-dependence, we assume that seed fertilization, seed number, and germination rate do not vary with climate.

³I think the supplement should also include a data figure showing the fit of the model to the experimental data.

The dynamics of the size-structured component of the population are given by:

$$F_{y,t+1} = [\sigma \cdot g^F(y, x=1)] F_t^R + \sum_L^U [s^F(x) \cdot g^F(y, x)] F_{x,t} \quad (4)$$

$$M_{y,t+1} = [\sigma \cdot g^M(y, x=1)] M_t^R + \sum_L^U [s^M(x) \cdot g^M(y, x)] M_{x,t} \quad (5)$$

231 The first terms indicate recruits that survived their first year and enter the size distribution
 232 of established plants. We estimated the seedling survival probability σ using demographic
 233 data from the congeneric species *Poa autumnalis* in east Texas (T.E.X. Miller and J.A. Rudgers,
 234 *unpublished data*), and we assume that σ is the same across sexes and climatic variables. We did
 235 this because we had little information on the early life cycle transitions of greenhouse-raised
 236 transplants. We used $g(y, x=1)$ (the future size distribution of one-tiller plants from the
 237 transplant experiment) to give the probability that a surviving recruit reaches size y . The
 238 second component of the equations indicates survival and size transition of established
 239 plants from the previous year, where s and g give the probabilities of surviving at size x and
 240 growing from sizes x to y , respectively, and superscripts indicate that these functions may
 241 be unique to females (F) and males (M).

242 The model described above yields a $2(U+1) \times 2(U+1)$ transition matrix. We estimated
 243 the population growth rate λ of the female dominant model as the leading eigenvalue of
 244 the transition matrix. Since the two-sex MPM is nonlinear (matrix elements affect and are
 245 affected by population structure) we estimated λ and stable sex ratio (female fraction of all
 246 individuals) and operational sex ratio (female fraction of panicles) by numerical simulation.
 247 Since all parameters were estimated using MCMC sampling, we were able to propagate the
 248 uncertainty in our estimates of the vital rate parameters to uncertainty in λ . Furthermore,
 249 by sampling over distributions associated with site, block, and source population variance
 250 terms, we are able to incorporate process error into the total uncertainty in λ , in addition
 251 to the uncertainty that arises from imperfect knowledge of the parameter values. For example,
 252 sampling over site and block variances accounts for regional and local spatial heterogeneity
 253 that is not explained by climate, and sampling over source population variance accounts for
 254 genetically-based demographic differences across the species' range.

255 Life Table Response Experiments

256 We conducted two types of Life Table Response Experiments (LTRE) to isolate contributions of
 257 climate variables and sex-specific vital rates to variation in λ . First, to identify which aspect of
 258 climate is most important for population viability, we used an LTRE based on a nonparametric

model for the dependence of λ on parameters associated with seasonal temperature and precipitation (Ellner et al., 2016). To do so, we used the RandomForest package to fit a regression model with four climatic variables (temperature of growing season, precipitation of growing season, temperature of the dormant season and precipitation of the dormant season) as predictors and λ calculated from the two sex model as response (Liaw et al., 2002). The regression model allowed the estimation of the relative importance of each predictor.

Second, to understand how climate drivers influence λ via sex-specific demography, we decomposed the effect of each climate variable on population growth rate (λ) into contribution arising from the effect on each female and male vital rate using a “regression design” LTRE (Caswell, 1989, 2000). This LTRE decomposes the sensitivity of λ to climate according to:

$$\frac{\partial \lambda}{\partial \text{climate}} \approx \sum_i \frac{\partial \lambda}{\partial \theta_i^F} \frac{\partial \theta_i^F}{\partial \text{climate}} + \frac{\partial \lambda}{\partial \theta_i^M} \frac{\partial \theta_i^M}{\partial \text{climate}} \quad (6)$$

where, θ_i^F and θ_i^M represent sex-specific parameters (the regression coefficients of the vital rate functions). Because LTRE contributions are additive, we summed across vital rates to compare the total contributions of female and male parameters.⁴⁵

Population viability across the climatic niche and geographic range

To understand how climate shapes the niche and geographic range of Texas bluegrass, we estimated the probability of self-sustaining populations ($\Pr(\lambda \geq 1)$) conditional to temperature and precipitation of the dormant and growing seasons. $\Pr(\lambda > 1)$ was calculated for the two-sex model and the female dominant MPMs using the proportion of the 300 posterior samples that lead to a $\lambda \geq 1$ (Diez et al., 2014). Population viability in climate niche space was then represented as a contour plot with values of $\Pr(\lambda > 1)$ at given temperature and precipitation for the growing season, holding dormant season climate constant, and vice versa.

$\Pr(\lambda > 1)$ was also mapped onto geographic layers of three US states (Texas, Oklahoma and Kansas) to delineate past, current and future potential geographic distribution of the species. To do so, we estimated $\Pr(\lambda > 1)$ conditional to all climate covariates for each pixel ($\sim 25 \text{ km}^2$) for each time period (past, present, future). Because of the amount of the computation involved, we use 100 posterior samples to estimate $\Pr(\lambda > 1)$ across the study area (Texas, Oklahoma and Kansas).

⁴Let's talk about this

⁵I do not agree. It is true that you can compute this, but only by “turning off” the interaction by holding the interacting variable constant. I still think this needs to be better addressed in both LTRE analyses.

286 **Results**

287 **Sex specific demographic responses and sex ratio variation across climatic
288 conditions**

289 We found strong demographic responses to climate drivers across our Texas bluegrass
290 common garden sites and years, and evidence for demographic differences between the
291 sexes. Regression coefficients related to sex and/or sex:size interactions were significantly
292 non-zero (95% credible intervals excluding zero) for most vital rates (Fig. S-4), suggesting
293 sexual divergence in demography. Females generally had an advantage over males, especially
294 in survival and flowering (Fig. 2). **Across all sites and years, % of females survived compared
295 to % of males, and % of surviving females flowered compared to % of surviving males.**⁶
296 Furthermore, there were significant interactions between sex and one or more climate
297 variables, particularly for growth (Fig. S-4B), indicating sexual niche divergence in response
298 to shared climate drivers. Figures S-5 and S-6 visualize the magnitude of sexual divergence
299 in demography across niche space, revealing that female advantages in flowering and panicle
300 production were greatest at both high and low growing season temperature extremes.

⁶*I think it would be interesting to add just the raw numbers here.*

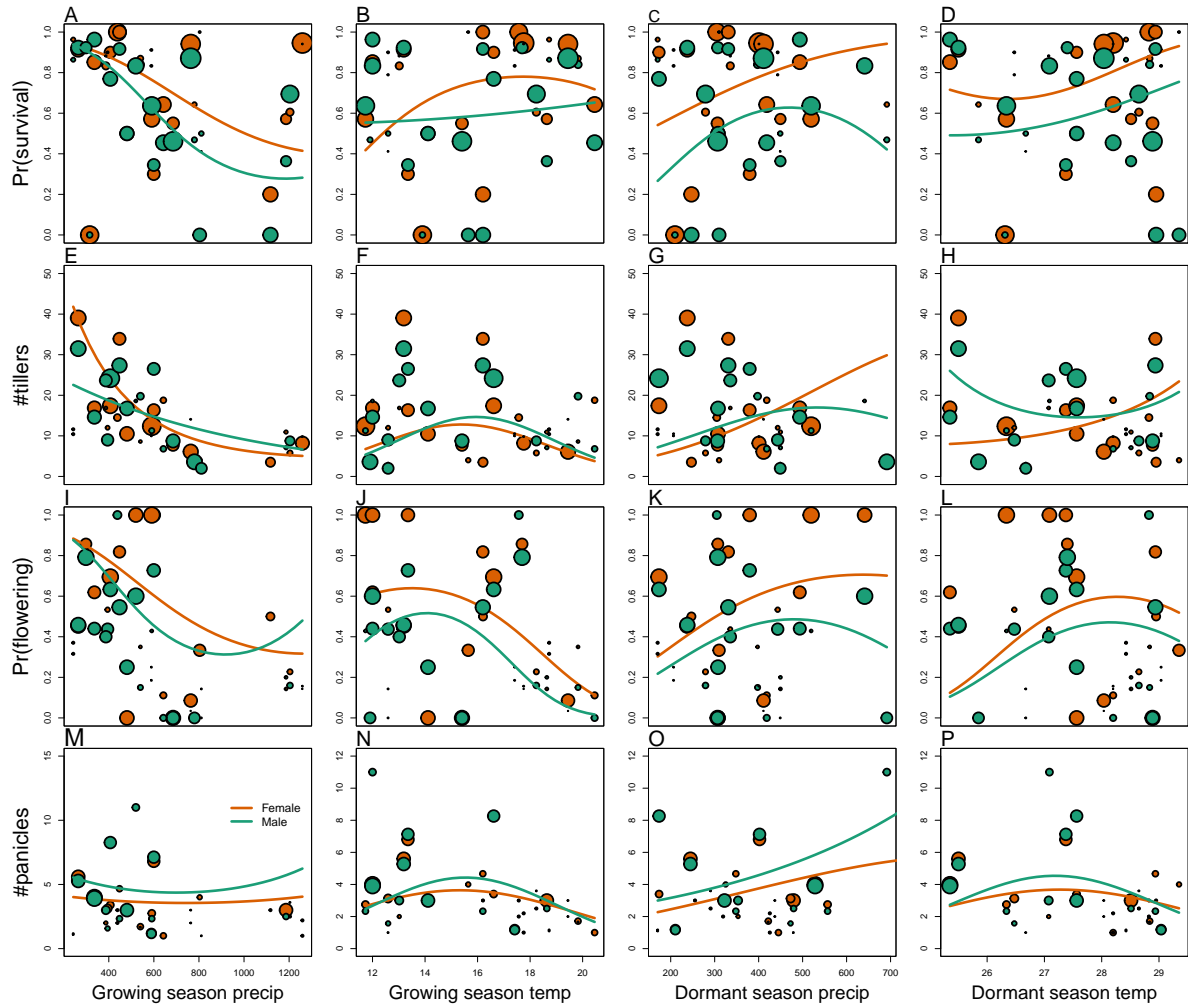


Figure 2: Sex specific demographic response to climate across species range. (A, B, C, D) Probability of survival as a function of precipitation and temperature of the growing and dormant season. (E, F, G, H) Change in number of tillers as a function of precipitation and temperature of the growing and dormant season. (I, J, K, L) Probability of flowering as a function of precipitation and temperature of growing and dormant season. (M, N, O, P) Change in number of panicles as a function of precipitation and temperature of the growing and dormant season. Points show means by site for females (orange) and males (green). Points sizes are proportional to the sample sizes of the mean and are jittered. Lines show fitted statistical models for females (orange) and males (green) based on posterior mean parameter values.

301 Across common garden sites, operational sex ratio (proportion of panicles that are female)
 302 of the experimental populations was female-biased on average ($\approx 60\%$ female), reflecting the
 303 overall greater rates of female vs. male flowering rather than bias in the underlying population
 304 composition. OSR was most female-biased (up to 80% female) at extreme values of tempera-
 305 ture, especially growing season temperature (Figure S-7, Figure S-8), consistent with the female
 306 reproductive advantage at temperature extremes seen in the vital rate data (Figure S-5). In
 307 contrast, there was very little variation in sex ratio (proportion of plants that are female) in the

308 years following common garden establishment (all sites were planted with equal numbers of fe-
309 males and males) and no detectable influence of climate covariates (Figure S-9), indicating that
310 skew in the OSR comes from sex-biased reproductive rates more so than sex-biased survival.

311 Climate drivers of population viability across niche space

312 Putting all vital rates together in the MPM framework reveals how climate shapes fitness
313 variation across niche dimensions and geographic space, and how accounting for sex structure
314 modifies these inferences. Figure 3 shows the estimated probability of population viability
315 ($\lambda \geq 1$) across seasonal climate niche space; these probabilities account for uncertainty in the
316 vital rate parameters as well as process error related to spatial heterogeneity and genotypic
317 variation. For both female-dominant and two-sex models, fitness variation across niche space
318 was dominated by temperature, with weaker effects of precipitation (compare vertical and
319 horizontal contours in Fig. 3). These visual trends are supported by LTRE decomposition
320 indicating that variation in fitness across climatic conditions is most strongly driven by
321 responses to growing and dormant season temperature, with weaker interactive effects of
322 precipitation that modulate the effects of temperature (Figure S-11). LTRE analysis also showed
323 that declines in population viability at high and low temperatures were driven most strongly
324 by reductions in vegetative growth and panicle production, with stronger contributions from
325 females than males (Figure S-12). Intermediate temperatures of both growing and dormant
326 seasons were associated with near-certain projections of population viability ($Pr(\lambda \geq 1) \approx 1$),
327 and high and low temperature extremes during both seasons were associated with low niche
328 suitability ($Pr(\lambda \geq 1) < 0.2$). Higher precipitation slightly expanded the range of suitable
329 temperatures during the dormant season (Fig. 3A), and the reverse was true in the growing
330 season (Fig. 3B). Points in Fig. 3 show that climate change forecasted for the common
331 garden locations would move many of them toward lower-suitability regions of niche space
332 associated with high growing and dormant season temperatures (see also Fig. S-13).

333 While the female-dominant and two-sex models were generally in agreement about high
334 confidence in intermediate temperature optima, they differed around the edges of niche space
335 (Fig. 3C,D,S-13). The female-dominant model over-predicted population viability, especially
336 with respect to growing season temperature. For example, the female-dominant model
337 predicted⁷ that, for most levels of precipitation, warm growing season (winter) temperatures
338 of $\sim 20^{\circ}\text{C}$ had high suitability ($Pr(\lambda \geq 1) > 0.9$), while the two-sex model indicated that these
339 conditions were most likely unsuitable ($Pr(\lambda \geq 1) < 0.5$). Similarly, at low winter temperatures
340 that the two-sex model identifies with high certainty as unsuitable ($Pr(\lambda \geq 1) < 0.1$), the

⁷ I think I am switching tenses. We will need to clean this up.

female-dominant model is more optimistic ($Pr(\lambda \geq 1) > 0.4$). Across growing season climate space, the female-dominant model over-estimates population viability by ca. 10%,⁸ on average (Fig. 3D, Fig. S-15B). The difference between female-dominant and two-sex models was qualitatively similar but weaker in magnitude for niche dimensions of the dormant season (Fig. 3C, Fig. S-15A).⁹ Female-dominant and two-sex models diverged most strongly in regions of niche space that favored strongly female-biased operational sex ratios (Figure S-16)¹⁰¹¹. This suggests mate limitation as the biological mechanism underlying model differences. The two-sex model accounts for feedbacks between OSR and female fertility, with reduced seed viability at OSR exceeding ~ 75% female panicles (Fig. WE NEED A FIGURE FOR THIS)^{12,13}. Lacking this feedback, the female-dominant model over-predicts population viability in regions of niche space where male flowering is not sufficient to maximize seed set.

⁸I would check what this difference actually is. The number 10 came from me guessing.

⁹The niche histogram figure is duplicated in the supplement. Also, can you add a legend to this figure?

¹⁰This Figure is new and I am not sure if we should keep it in the manuscript

¹¹I like it! But is the scale correct on panel A?

¹²I don't understand the type of Figure you are asking here

¹³I am talking about a figure showing how seed viability declines with increasing female bias in the OSR. This could go in th section of the supplement where you describe that experiment and analysis.

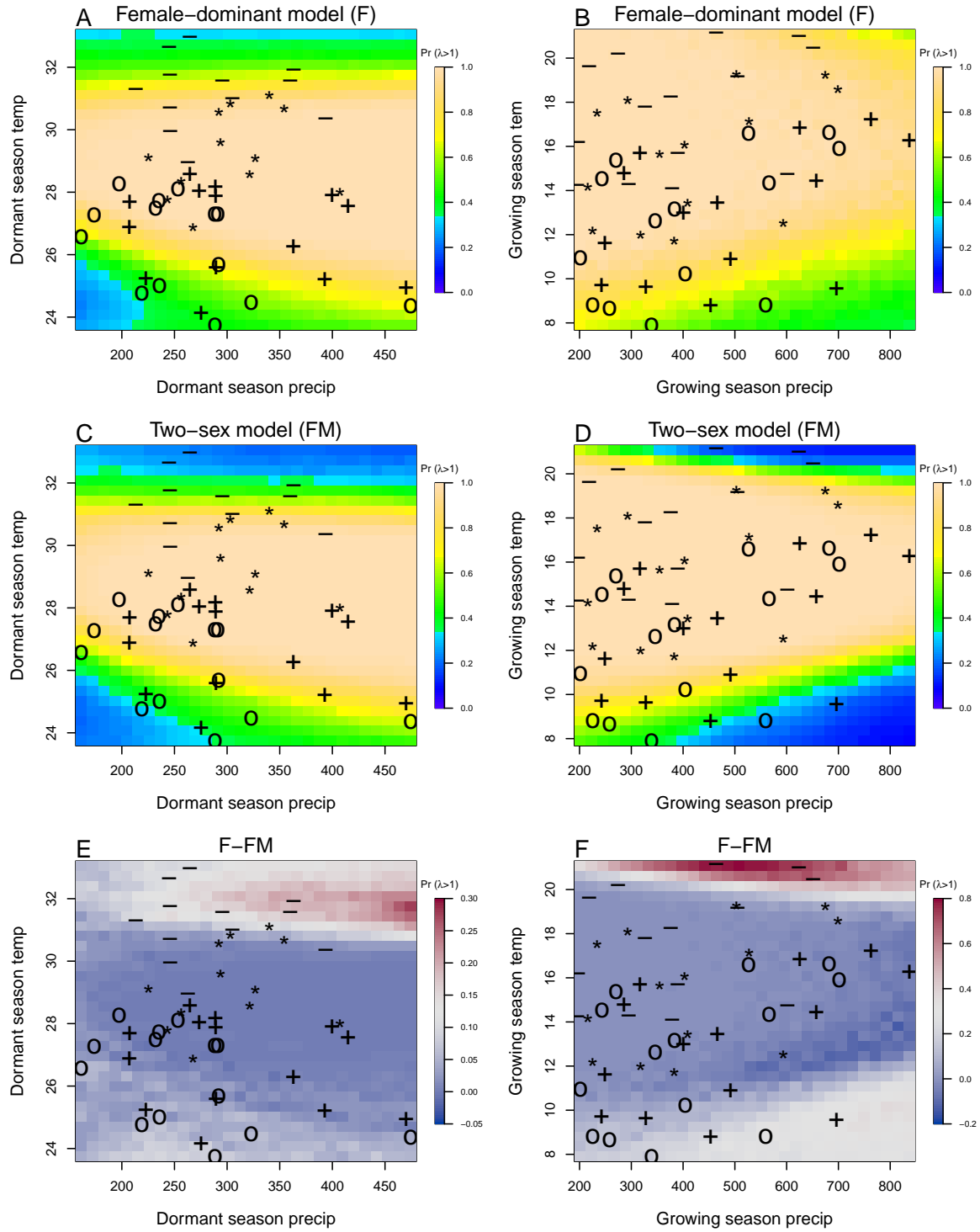


Figure 3: A two-dimensional representation of the predicted niche shift over time (past, present and future climate conditions). "O": Past, "+" Current, "*": RCP 4.5, "-": RCP 8.5.

352 **Climatic change induces shifts in geographic niche and population OSR**

353 Projecting the climatic niche onto geographic space, we find that suitable niche conditions for
354 Texas bluegrass are shifting north under climate change (Fig. 4). Under past (1901-1930) and
355 present (1990-2019) conditions, the two-sex and female-dominant models predict widespread
356 suitability with high confidence ($Pr(\lambda \geq 1) \approx 1$) across much of Texas and Oklahoma. For
357 both models, the predicted geographic niche generally corresponds well to independent
358 observations of the Texas bluegrass distribution (Fig. 4). The predicted geographic niche is
359 more expansive than the GBIF occurrences, particularly at southern, western, and eastern
360 edges, suggesting some degree of range disequilibrium (e.g., due to dispersal limitation),
361 geographic bias in occurrence records, and/or model mis-specification. Comparing past
362 to present conditions, the geographic niche for both models has shifted slightly poleward,
363 with reductions in viability at the southern margins and expansions of viability at northern
364 margins. The northward shift of suitable niche conditions is even more pronounced in
365 projections to end-of-century (2071-2100) conditions, with the most dramatic changes in the
366 most pessimistic (RCP8.5) scenario (Fig. 4.¹⁴¹⁵). In fact, under the pessimistic scenario, Texas
367 bluegrass will have very little remaining climate suitability in the state of Texas by the end
368 of the 21st century. The predicted poleward niche shift is consistent across different global
369 circulation models (Figure S-17, Figure S-18, Figure S-19).

370 Female-dominant and two-sex models are in broad agreement about northward
371 migration of the climatic niche, but the geographic projections reveal hotspots of disagreement
372 where the female-dominant model over-predicts climate suitability and under-predicts the
373 likelihood of range shifts (Fig. 4). These hotspots are generally regions of predicted female
374 bias in the operational sex ratio (Figure 6).¹⁶ The strongest contrast between the two models
375 is in the pessimistic climate change scenario (RCP8.5), where the female-dominant model
376 over-predicts population viability by as much as 20% across much of the region (Figure
377 S-20) and thus under-estimates the magnitude of a potential range shift. In this scenario,
378 a broad swath of the current distribution that is forecasted to be effectively unsuitable
379 ($Pr(\lambda \geq 1) \approx 0$) by the two-sex model is identified as marginally suitable ($Pr(\lambda \geq 1) \approx 0.5$)
380 by the female-dominant model. Accordingly, the OSR of Texas bluegrass across its range
381 is projected to be ca. 75% female panicles, on average, by end of century under RCP8.5, an
382 increase from ca. 60% female under projections for past and current conditions (Fig. 5). The

¹⁴I am not sure if we need a title for each panel.

¹⁵I am not sure what you are asking but I like the figure as it is. But you can remove one of the two lambda color ramps, since they are the same.

¹⁶I really like this figure but it might work better as a supplement figure--let's discuss. It suggests for example that the range size will actually increase under RCP4.5. You also need to update the legend.

³⁸³ more optimistic climate change scenario (RCP4.5) predicts an intermediate shift in OSR, with
³⁸⁴ hotspots of change at northern and southern range edges becoming strongly female-biased
³⁸⁵ but most of the range remaining near current levels of 60% female (Fig. 5; Fig. 6).

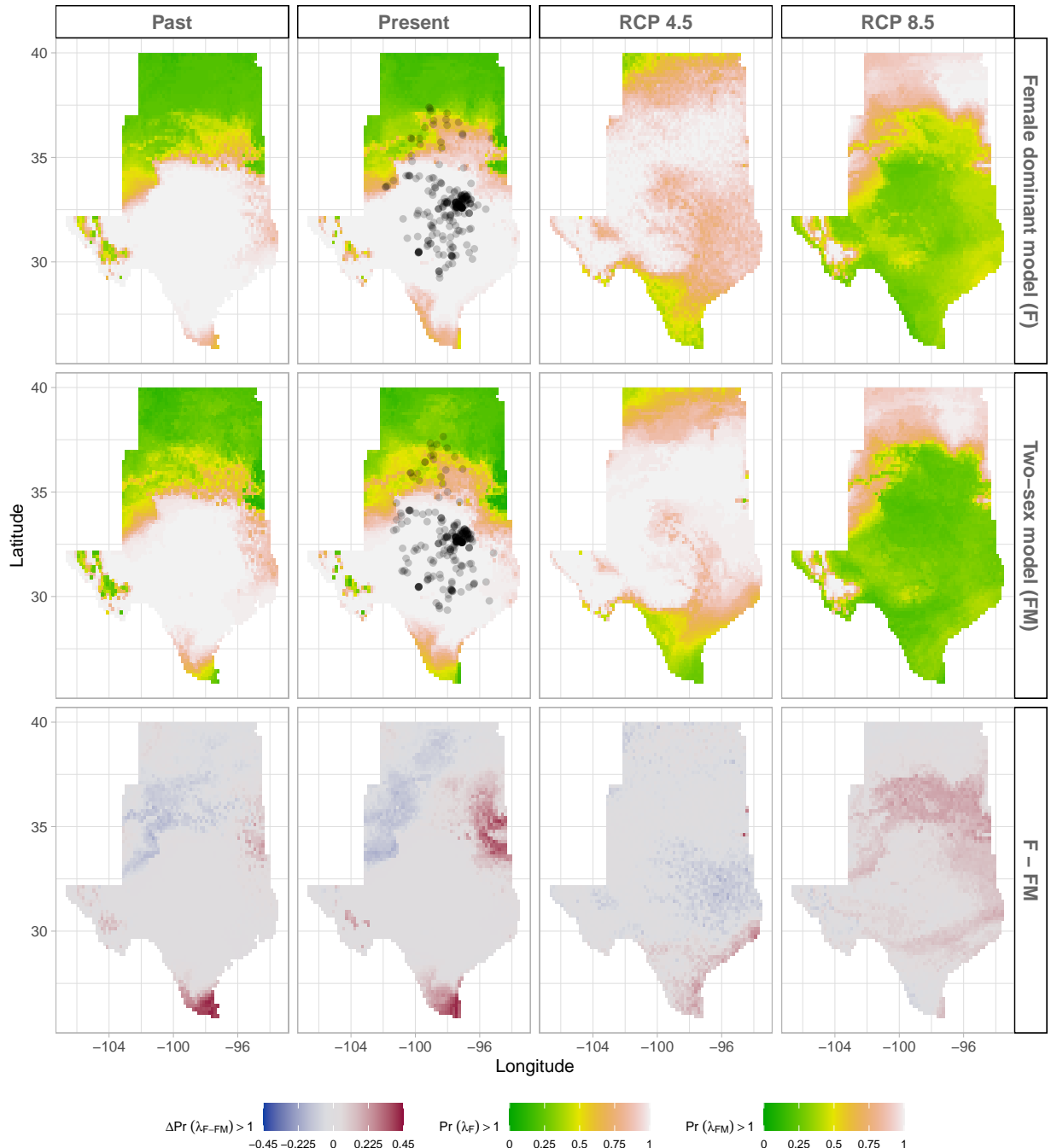


Figure 4: Climate change favors range shift towards north edge. (A) Past, (B) Current, (C and D) Future predicted range shift based on the predicted probabilities of self- sustaining populations, $\text{Pr}(\lambda > 1)$, using the two-sex model that incorporates sex- specific demographic responses to climate with sex ratio dependent seed fertilization. (E) Past, (F) Current, (G and H) Future predicted range shift based on the predicted probabilities of self- sustaining populations, $\text{Pr}(\lambda > 1)$, using the female dominant model. Future projections were based on the CMCC-CM model. The black dots on panel B and F indicate all known presence points collected from GBIF. The occurrences of GBIFs are distributed in with higher population fitness habitat $\text{Pr}(\lambda > 1)$, confirming that our study approach can reasonably predict range shifts.

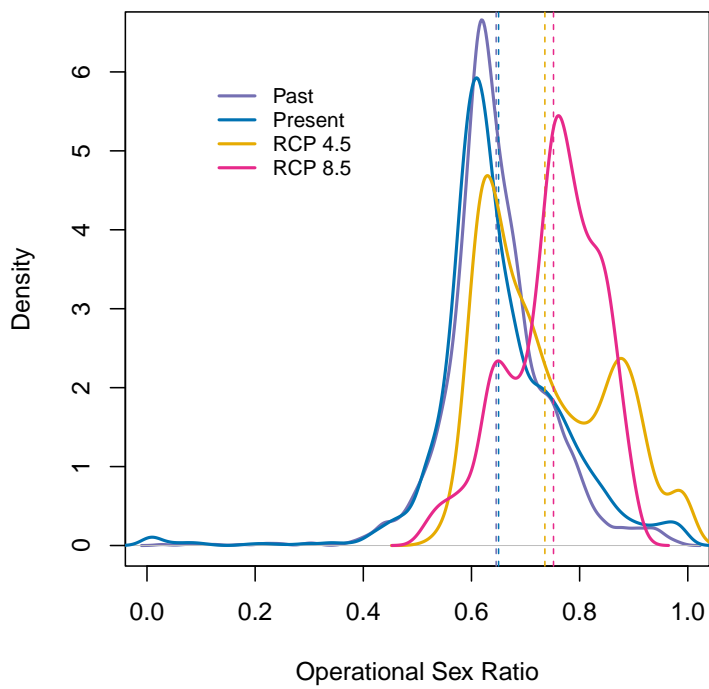


Figure 5: Change in Operational Sex Ratio (proportion of female panicle) over time (past, present, future). Future projections were based on the CMCC-CM model. The mean sex ratio for each time period is shown as vertical dashed line.

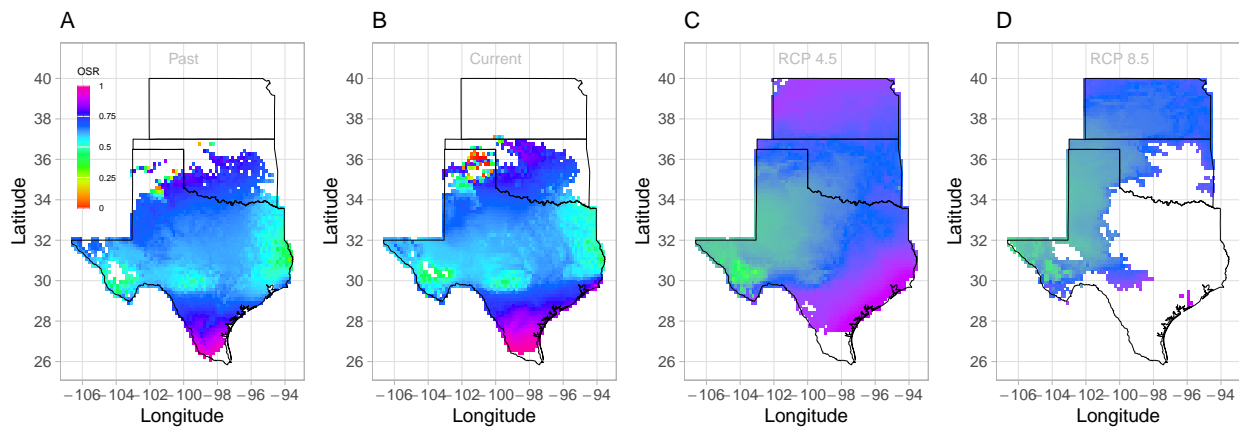


Figure 6: Change in Operational Sex Ratio (proportion of female panicle) over time (past, present, future) across species range. Future projections were based on the CMCC-CM model. The mean sex ratio for each time period is shown as vertical dashed line.

386 **Discussion**

387 Dioecious species make up a large fraction of Earth's biodiversity – most animals and many
388 plants – yet we have little knowledge about how sex-specific demography and responses to
389 climate drivers may affect population viability and range shifts of dioecious species under
390 climate change. We used demographic data collected from common garden experiments,
391 hierarchical Bayesian statistical modeling, and sex-structured demographic modeling to
392 forecast for the first time the likely impact of climate change on range dynamics of a dioecious
393 species. We found that demographic rates of Texas bluegrass and their sensitivities to climate
394 drivers show significant sex bias, with females out-performing males, on average, and high
395 and low temperature extremes disproportionately favoring female reproduction, leading to
396 female skew in the operational sex ratio. In fact, we show that future climate change will likely
397 not only shift this species' geographic niche northward, but it will also skew operational sex
398 ratios toward stronger female bias. Our two-sex modeling framework accounts for reductions
399 in female fertility with increasing female bias, and therefore predicts a narrower climatic niche
400 than the corresponding female-dominant model that ignores the feedback between population
401 structure and vital rates. Failure to account for population sex structure can therefore lead to
402 overestimation of suitable niche space and underestimation of range shifts under global change.

403 ¹⁷Our finding that climate change in the south-central US will likely lead to female-biased
404 operational sex ratios contrasts with previous studies of dioecious plants. While a baseline
405 female demographic advantage has been observed in several dioecious species (Sasaki et al.,
406 2019; Welbergen et al., 2008; Zhao et al., 2012), **studies**¹⁸ focused on sex-specific sensitivity to
407 climate drivers predict an increase in male frequency in response to climate change (Hultine
408 et al., 2016; Petry et al., 2016). We speculate that differences in the costs of reproduction
409 related to pollination mode may help explain which sex is favored under climate stress. For
410 most dioecious plant species, the cost of reproduction is often higher for females than males
411 due to the requirement to develop seeds and fruits (Hultine et al., 2016). However, several
412 studies reported a higher cost of reproduction for males in wind pollinated species due to
413 the larger amounts of pollen they produce (Brujning et al., 2017; Bürl et al., 2022; Cipollini
414 and Whigham, 1994; Field et al., 2013). **Additional comparative studies across species that**

¹⁷I like this paragraph. I would probably try to incorporate some older literature on costs of reproduction in dioecious plants. There are some classic papers from the 80s. There are also some papers by Sarah Eppley showing female advantage in grasses. I may not have understood the point you were trying to make about life history traits.

¹⁸Are there more than just these two citations? This is good motivation to finish our meta-analysis!

415 differ in life history traits are needed to draw inferences regarding which types of species
416 are likely to become female- or male-biased in response to global change stressors.¹⁹

417 While a two-sex modeling approach clearly adds biological realism, it was also additional
418 work (in the form of experiments, data, equations, code, and computation). Was it worth
419 the trouble? Generally, we suggest the answer should depend on the aims of the investigator.
420 Predictions of the sex-structured and female-dominant models were in strong agreement
421 about climate niche optima, and LTRE decomposition suggested that female vital rates
422 determine population responses to climate variation much more so than male vital rates.
423 If we wanted to know whether a poleward range shift is likely for Texas bluegrass, the
424 simpler female-dominant approach could have given us the correct answer. But more focused
425 questions, especially around the edges of niche space where sex ratio skew is more likely to
426 impair population viability, may require an explicit accounting for sex structure. If we aimed
427 to identify specific regions that are more or less inclined toward contraction or expansion,
428 or sites that might be suitable for assisted migration, we might reach qualitatively different
429 conclusions with female-dominant and two-sex models. For example, the female-dominant
430 model is over-confident that large swaths of Oklahoma will remain marginally suitable for
431 Texas bluegrass under the business-as-usual emissions scenario, while the two-sex model
432 is more pessimistic, because this region will become too female-biased to support viable
433 populations. More generally, we hypothesize that accounting for sex structure should be most
434 important under conditions that are already near the limits of population viability, where
435 effects of mate limitation could be more consequential. This suggests a particularly important
436 role of sex-structured modeling for threatened and endangered species, as conservation
437 biologists have already recognized (cite Taiga antelope, penguins, polar bears).

438 Our results suggest that climate change, and specifically climate warming, will
439 drive a classic pattern of poleward expansion: contraction at the southern trailing edge
440 due to temperatures exceeding tolerable limits and expansion at the northern leading
441 edge due to release from low temperature limitation. Our statistical models captured
442 temperature-dependence in a phenomenological way, and the physiological mechanisms
443 underlying these responses remain to be explored. Increasing temperature could increase
444 evaporative demand, affect plant phenology (Iler et al., 2019; McLean et al., 2016; Sherry et al.,
445 2007), and germination rate (Reed et al., 2021). The potential for temperature to influence
446 these different processes changes seasonally (Konapala et al., 2020). For example, studies
447 suggested that species that are active during the growing season such as cool grass species

¹⁹Notice that I usually try to have each paragraph of the discussion end with a sentence that provides some synthesis of the ideas covered in the paragraph and/or identifies some direction for next steps. That is one of my strategies for writing a Discussion.

448 can have delayed phenology in response to global warming, particularly if temperatures rise
449 above their physiological tolerances (Cleland et al., 2007; Williams et al., 2015).

450 Regardless of the mechanism, it is clear that climate warming will generate leading and
451 trailing edges. Whether and at what pace the realized species' distribution tracks geographic
452 changes in suitable niche space is a different, open question. Expansion of the leading
453 edge could lag behind availability of suitable habitat due to dispersal limitation (cite), and
454 legacies of long-lived individuals can promote persistence of trailing edge populations even
455 as environmental conditions deteriorate (cite nice tree paper). ²⁰ Environmentally-explicit
456 demographic models are emerging as powerful tools to understand and predicts the limits
457 of population viability under global change (Schultz et al., Merow et al.), but incorporating
458 non-equilibrium dynamics that emerge from dispersal limitation and and historical legacies
459 is an important new direction for this field.²¹

460 Our forecasts for responses to climate change in Texas bluegrass should be interpreted
461 in light of several features²² of our study design. First, the design of our common garden
462 experiment and statistical modeling means that our geographic projections correspond to an
463 "average" genotype from across the range of Texas bluegrass. Local adaptation to climate could
464 make southern and northern edge populations more resilient to high and low temperature
465 stress, respectively, than the range-wide average (cite). The role of local adaptation in
466 mitigating population response to climate is an important next step in forecasting species'
467 responses to global change (cite). Second, as is true for many ecological systems, future
468 climate is likely to include conditions that have no present-day analog (cite), a major challenge
469 for ecological forecasting. The years and locations of our experiment provided us with
470 unusually good coverage of likely past, present, and future conditions expected throughout
471 the study region, but we still had to extrapolate the statistical models to predict responses
472 to colder winter temperatures (that were more common in the past) and hotter summer
473 temperatures (that are expected in the future) than we directly observed (Fig. 1). By employing
474 a probabilistic measure of niche and geographic suitability ($Pr(\lambda) \geq 1$), our projections
475 account for the uncertainty associated with these extrapolated climate responses, but there
476 would be value in combining the spatiotemporal sampling of a common garden design with
477 experimental manipulations that push systems toward historical and/or future conditions
478 (cite). Third, while we incorporated uncertainty associated with parameter estimation and

²⁰It would be really interesting to ask how long we expect southern edge populations to persist. I think we can quantify this with the model! Maybe for the next paper.

²¹This would be good content for an opinion paper! And this reminds me of a talk I saw at ESA a few years ago that did this with fish. Do you know if that is published. I can look up the author.

²²Something I thought about including here (but did not because of concern about length) is the fact that the model greatly overpredicts the GBIF occurrences. What do you think that means for our forecasts? WOULD this bias the forecast in one direction or another?

479 process error, there is additional uncertainty in future climate conditions. Future forecasts for
480 Texas bluegrass were generally consistent across different global circulation models (reference
481 supp figures), but combining uncertainty in future conditions alongside uncertainty in
482 biological responses to those conditions is an important frontier in ecological forecasting (cite).

483 Conclusion

484 We investigated how demographic differences between the sexes and contrasting sensitivity to
485 climate can drive skewness in sex ratio on and possible range shifts in the context of climate
486 change. For Texas bluegrass, the future is female, and it is in Kansas. Our results suggest
487 that tracking only females could lead to an underestimation of the effect of climate change
488 on population dynamics, because it misses the feedback between population structure and
489 female fertility. But in broad strokes, a female-dominant perspective tells much of the story,
490 and that will likely be true for dioecious plants and animals with mating systems in which
491 few males can fertilize many females. Our work also provides a framework for predicting
492 the impact of global change on population dynamics and range shifts using probabilistic
493 measures that can incorporate and pick apart the many types of uncertainty that arise when
494 reconstructing the past or forecasting the future.

495 Acknowledgements

496 This research was supported by National Science Foundation Division of Environmental
497 Biology awards 2208857 and 2225027. We thank the organizations and institutions who hosted
498 us at their field station facilities, including The Nature Conservancy, Sam Houston State
499 University, University of Texas, Texas A&M University, Texas Tech University, Lake Lewisville
500 Environmental Learning Area, Wichita State University, and Pittsburgh State University.

501 **References**

- 502 Bertrand, R., Lenoir, J., Piedallu, C., Riofrío-Dillon, G., De Ruffray, P., Vidal, C., Pierrat, J.-C.,
503 and Gégout, J.-C. (2011). Changes in plant community composition lag behind climate
504 warming in lowland forests. *Nature*, 479(7374):517–520.
- 505 Bruijning, M., Visser, M. D., Muller-Landau, H. C., Wright, S. J., Comita, L. S., Hubbell, S. P.,
506 de Kroon, H., and Jongejans, E. (2017). Surviving in a cosexual world: A cost-benefit
507 analysis of dioecy in tropical trees. *The American Naturalist*, 189(3):297–314.
- 508 Bürli, S., Pannell, J. R., and Tonnabel, J. (2022). Environmental variation in sex ratios and
509 sexual dimorphism in three wind-pollinated dioecious plant species. *Oikos*, 2022(6):e08651.
- 510 Caswell, H. (1989). Analysis of life table response experiments i. decomposition of effects
511 on population growth rate. *Ecological Modelling*, 46(3-4):221–237.
- 512 Caswell, H. (2000). *Matrix population models*, volume 1. Sinauer Sunderland, MA.
- 513 Cipollini, M. L. and Whigham, D. F. (1994). Sexual dimorphism and cost of reproduction
514 in the dioecious shrub *lindera benzoin* (lauraceae). *American Journal of Botany*, 81(1):65–75.
- 515 Cleland, E. E., Chuine, I., Menzel, A., Mooney, H. A., and Schwartz, M. D. (2007). Shifting
516 plant phenology in response to global change. *Trends in ecology & evolution*, 22(7):357–365.
- 517 Compagnoni, A., Steigman, K., and Miller, T. E. (2017). Can't live with them, can't live
518 without them? balancing mating and competition in two-sex populations. *Proceedings of
519 the Royal Society B: Biological Sciences*, 284(1865):20171999.
- 520 Czachura, K. and Miller, T. E. (2020). Demographic back-casting reveals that subtle
521 dimensions of climate change have strong effects on population viability. *Journal of Ecology*,
522 108(6):2557–2570.
- 523 Dahlgren, J. P., Bengtsson, K., and Ehrlén, J. (2016). The demography of climate-driven and
524 density-regulated population dynamics in a perennial plant. *Ecology*, 97(4):899–907.
- 525 Davis, M. B. and Shaw, R. G. (2001). Range shifts and adaptive responses to quaternary
526 climate change. *Science*, 292(5517):673–679.
- 527 Diez, J. M., Giladi, I., Warren, R., and Pulliam, H. R. (2014). Probabilistic and spatially variable
528 niches inferred from demography. *Journal of ecology*, 102(2):544–554.

- 529 Eberhart-Phillips, L. J., Küpper, C., Miller, T. E., Cruz-López, M., Maher, K. H., Dos Remedios,
530 N., Stoffel, M. A., Hoffman, J. I., Krüger, O., and Székely, T. (2017). Sex-specific early
531 survival drives adult sex ratio bias in snowy plovers and impacts mating system and
532 population growth. *Proceedings of the National Academy of Sciences*, 114(27):E5474–E5481.
- 533 Ehrlén, J. and Morris, W. F. (2015). Predicting changes in the distribution and abundance
534 of species under environmental change. *Ecology letters*, 18(3):303–314.
- 535 Elderd, B. D. and Miller, T. E. (2016). Quantifying demographic uncertainty: Bayesian methods
536 for integral projection models. *Ecological Monographs*, 86(1):125–144.
- 537 Ellis, R. P., Davison, W., Queirós, A. M., Kroeker, K. J., Calosi, P., Dupont, S., Spicer, J. I.,
538 Wilson, R. W., Widdicombe, S., and Urbina, M. A. (2017). Does sex really matter? explaining
539 intraspecies variation in ocean acidification responses. *Biology letters*, 13(2):20160761.
- 540 Ellner, S. P., Adler, P. B., Childs, D. Z., Hooker, G., Miller, T. E., and Rees, M. (2022). A critical
541 comparison of integral projection and matrix projection models for demographic analysis:
542 Comment. *Ecology*.
- 543 Ellner, S. P., Childs, D. Z., Rees, M., et al. (2016). Data-driven modelling of structured
544 populations. *A practical guide to the Integral Projection Model*. Cham: Springer.
- 545 Evans, M. E., Merow, C., Record, S., McMahon, S. M., and Enquist, B. J. (2016). Towards
546 process-based range modeling of many species. *Trends in Ecology & Evolution*, 31(11):860–871.
- 547 Field, D. L., Pickup, M., and Barrett, S. C. (2013). Comparative analyses of sex-ratio variation
548 in dioecious flowering plants. *Evolution*, 67(3):661–672.
- 549 Gamelon, M., Grøtan, V., Nilsson, A. L., Engen, S., Hurrell, J. W., Jerstad, K., Phillips, A. S.,
550 Røstad, O. W., Slagsvold, T., Walseng, B., et al. (2017). Interactions between demography
551 and environmental effects are important determinants of population dynamics. *Science
552 Advances*, 3(2):e1602298.
- 553 Gerber, L. R. and White, E. R. (2014). Two-sex matrix models in assessing population viability:
554 when do male dynamics matter? *Journal of Applied Ecology*, 51(1):270–278.
- 555 Gissi, E., Bowyer, R. T., and Bleich, V. C. (2024). Sex-based differences affect conservation.
556 *Science*, 384(6702):1309–1310.
- 557 Gissi, E., Schiebinger, L., Hadly, E. A., Crowder, L. B., Santoleri, R., and Micheli, F. (2023).
558 Exploring climate-induced sex-based differences in aquatic and terrestrial ecosystems to
559 mitigate biodiversity loss. *nature communications*, 14(1):4787.

- 560 Haridas, C., Eager, E. A., Rebarber, R., and Tenhumberg, B. (2014). Frequency-dependent
561 population dynamics: Effect of sex ratio and mating system on the elasticity of population
562 growth rate. *Theoretical Population Biology*, 97:49–56.
- 563 Hernández, C. M., Ellner, S. P., Adler, P. B., Hooker, G., and Snyder, R. E. (2023). An exact
564 version of life table response experiment analysis, and the r package exactltre. *Methods*
565 in Ecology and Evolution
- 566 Hitchcock, A. S. (1971). *Manual of the grasses of the United States*, volume 2. Courier Corporation.
- 567 Hultine, K. R., Grady, K. C., Wood, T. E., Shuster, S. M., Stella, J. C., and Whitham, T. G. (2016).
568 Climate change perils for dioecious plant species. *Nature Plants*, 2(8):1–8.
- 569 Iler, A. M., Compagnoni, A., Inouye, D. W., Williams, J. L., CaraDonna, P. J., Anderson, A., and
570 Miller, T. E. (2019). Reproductive losses due to climate change-induced earlier flowering are
571 not the primary threat to plant population viability in a perennial herb. *Journal of Ecology*,
572 107(4):1931–1943.
- 573 Jones, M. H., Macdonald, S. E., and Henry, G. H. (1999). Sex-and habitat-specific responses
574 of a high arctic willow, *salix arctica*, to experimental climate change. *Oikos*, pages 129–138.
- 575 Karger, D. N., Conrad, O., Böhner, J., Kawohl, T., Kreft, H., Soria-Auza, R. W., Zimmermann,
576 N. E., Linder, H. P., and Kessler, M. (2017). Climatologies at high resolution for the earth’s
577 land surface areas. *Scientific data*, 4(1):1–20.
- 578 Kindiger, B. (2004). Interspecific hybrids of *poa arachnifera* × *poa secunda*. *Journal of New*
579 *Seeds*, 6(1):1–26.
- 580 Knight, T. M., Steets, J. A., Vamosi, J. C., Mazer, S. J., Burd, M., Campbell, D. R., Dudash,
581 M. R., Johnston, M. O., Mitchell, R. J., and Ashman, T.-L. (2005). Pollen limitation of plant
582 reproduction: pattern and process. *Annu. Rev. Ecol. Evol. Syst.*, 36:467–497.
- 583 Konapala, G., Mishra, A. K., Wada, Y., and Mann, M. E. (2020). Climate change will affect
584 global water availability through compounding changes in seasonal precipitation and
585 evaporation. *Nature communications*, 11(1):3044.
- 586 Lee-Yaw, J. A., Kharouba, H. M., Bontrager, M., Mahony, C., Csergő, A. M., Noreen, A. M.,
587 Li, Q., Schuster, R., and Angert, A. L. (2016). A synthesis of transplant experiments and
588 ecological niche models suggests that range limits are often niche limits. *Ecology letters*,
589 19(6):710–722.

- 590 Liaw, A., Wiener, M., et al. (2002). Classification and regression by randomforest. *R news*,
591 2(3):18–22.
- 592 Louthan, A. M., Keighron, M., Kiekebusch, E., Cayton, H., Terando, A., and Morris, W. F.
593 (2022). Climate change weakens the impact of disturbance interval on the growth rate of
594 natural populations of venus flytrap. *Ecological Monographs*, 92(4):e1528.
- 595 Lynch, H. J., Rhainds, M., Calabrese, J. M., Cantrell, S., Cosner, C., and Fagan, W. F. (2014).
596 How climate extremes—not means—define a species' geographic range boundary via a
597 demographic tipping point. *Ecological Monographs*, 84(1):131–149.
- 598 McLean, N., Lawson, C. R., Leech, D. I., and van de Pol, M. (2016). Predicting when climate-
599 driven phenotypic change affects population dynamics. *Ecology Letters*, 19(6):595–608.
- 600 Merow, C., Bois, S. T., Allen, J. M., Xie, Y., and Silander Jr, J. A. (2017). Climate change both
601 facilitates and inhibits invasive plant ranges in new england. *Proceedings of the National
602 Academy of Sciences*, 114(16):E3276–E3284.
- 603 Miller, T. and Compagnoni, A. (2022a). Data from: Two-sex demography, sexual niche
604 differentiation, and the geographic range limits of texas bluegrass (*Poa arachnifera*). *American
605 Naturalist, Dryad Digital Repository*,. <https://doi.org/10.5061/dryad.kkwh70s5x>.
- 606 Miller, T. E. and Compagnoni, A. (2022b). Two-sex demography, sexual niche differentiation,
607 and the geographic range limits of texas bluegrass (*poa arachnifera*). *The American
608 Naturalist*, 200(1):17–31.
- 609 Miller, T. E., Shaw, A. K., Inouye, B. D., and Neubert, M. G. (2011). Sex-biased dispersal and
610 the speed of two-sex invasions. *The American Naturalist*, 177(5):549–561.
- 611 Morrison, C. A., Robinson, R. A., Clark, J. A., and Gill, J. A. (2016). Causes and consequences
612 of spatial variation in sex ratios in a declining bird species. *Journal of Animal Ecology*,
613 85(5):1298–1306.
- 614 Pease, C. M., Lande, R., and Bull, J. (1989). A model of population growth, dispersal and
615 evolution in a changing environment. *Ecology*, 70(6):1657–1664.
- 616 Petry, W. K., Soule, J. D., Iler, A. M., Chicas-Mosier, A., Inouye, D. W., Miller, T. E., and
617 Mooney, K. A. (2016). Sex-specific responses to climate change in plants alter population
618 sex ratio and performance. *Science*, 353(6294):69–71.

- 619 Piiroinen, J. and Vehtari, A. (2017). Comparison of bayesian predictive methods for model
620 selection. *Statistics and Computing*, 27:711–735.
- 621 Pottier, P., Burke, S., Drobniak, S. M., Lagisz, M., and Nakagawa, S. (2021). Sexual (in) equality?
622 a meta-analysis of sex differences in thermal acclimation capacity across ectotherms.
623 *Functional Ecology*, 35(12):2663–2678.
- 624 R Core Team (2023). *R: A Language and Environment for Statistical Computing*. R Foundation
625 for Statistical Computing, Vienna, Austria.
- 626 Reed, P. B., Peterson, M. L., Pfeifer-Meister, L. E., Morris, W. F., Doak, D. F., Roy, B. A., Johnson,
627 B. R., Bailes, G. T., Nelson, A. A., and Bridgman, S. D. (2021). Climate manipulations
628 differentially affect plant population dynamics within versus beyond northern range limits.
629 *Journal of Ecology*, 109(2):664–675.
- 630 Renganayaki, K., Jessup, R., Burson, B., Hussey, M., and Read, J. (2005). Identification of
631 male-specific aflu markers in dioecious texas bluegrass. *Crop science*, 45(6):2529–2539.
- 632 Sanderson, B. M., Knutti, R., and Caldwell, P. (2015). A representative democracy to reduce
633 interdependency in a multimodel ensemble. *Journal of Climate*, 28(13):5171–5194.
- 634 Sasaki, M., Hedberg, S., Richardson, K., and Dam, H. G. (2019). Complex interactions
635 between local adaptation, phenotypic plasticity and sex affect vulnerability to warming
636 in a widespread marine copepod. *Royal Society open science*, 6(3):182115.
- 637 Schultz, E. L., Hülsmann, L., Pillet, M. D., Hartig, F., Breshears, D. D., Record, S., Shaw, J. D.,
638 DeRose, R. J., Zuidema, P. A., and Evans, M. E. (2022). Climate-driven, but dynamic and
639 complex? a reconciliation of competing hypotheses for species' distributions. *Ecology letters*,
640 25(1):38–51.
- 641 Schwalm, C. R., Glendon, S., and Duffy, P. B. (2020). Rcp8. 5 tracks cumulative co2 emissions.
642 *Proceedings of the National Academy of Sciences*, 117(33):19656–19657.
- 643 Schwinning, S., Lortie, C. J., Esque, T. C., and DeFalco, L. A. (2022). What common-garden
644 experiments tell us about climate responses in plants.
- 645 Sexton, J. P., McIntyre, P. J., Angert, A. L., and Rice, K. J. (2009). Evolution and ecology of
646 species range limits. *Annu. Rev. Ecol. Evol. Syst.*, 40:415–436.
- 647 Shelton, A. O. (2010). The ecological and evolutionary drivers of female-biased sex ratios:
648 two-sex models of perennial seagrasses. *The American Naturalist*, 175(3):302–315.

- 649 Sherry, R. A., Zhou, X., Gu, S., Arnone III, J. A., Schimel, D. S., Verburg, P. S., Wallace,
650 L. L., and Luo, Y. (2007). Divergence of reproductive phenology under climate warming.
651 *Proceedings of the National Academy of Sciences*, 104(1):198–202.
- 652 Sletvold, N., Dahlgren, J. P., Øien, D.-I., Moen, A., and Ehrlén, J. (2013). Climate warming
653 alters effects of management on population viability of threatened species: results from
654 a 30-year experimental study on a rare orchid. *Global Change Biology*, 19(9):2729–2738.
- 655 Smith, M. D., Wilkins, K. D., Holdrege, M. C., Wilfahrt, P., Collins, S. L., Knapp, A. K., Sala,
656 O. E., Dukes, J. S., Phillips, R. P., Yahdjian, L., et al. (2024). Extreme drought impacts have
657 been underestimated in grasslands and shrublands globally. *Proceedings of the National
658 Academy of Sciences*, 121(4):e2309881120.
- 659 Stan Development Team (2023). RStan: the R interface to Stan. R package version 2.21.8.
- 660 Thomson, A. M., Calvin, K. V., Smith, S. J., Kyle, G. P., Volke, A., Patel, P., Delgado-Arias,
661 S., Bond-Lamberty, B., Wise, M. A., Clarke, L. E., et al. (2011). Rcp4. 5: a pathway for
662 stabilization of radiative forcing by 2100. *Climatic change*, 109:77–94.
- 663 Tognetti, R. (2012). Adaptation to climate change of dioecious plants: does gender balance
664 matter? *Tree Physiology*, 32(11):1321–1324.
- 665 Welbergen, J. A., Klose, S. M., Markus, N., and Eby, P. (2008). Climate change and the
666 effects of temperature extremes on australian flying-foxes. *Proceedings of the Royal Society
667 B: Biological Sciences*, 275(1633):419–425.
- 668 Williams, J. L., Jacquemyn, H., Ochocki, B. M., Brys, R., and Miller, T. E. (2015). Life
669 history evolution under climate change and its influence on the population dynamics of
670 a long-lived plant. *Journal of Ecology*, 103(4):798–808.
- 671 Zhao, H., Li, Y., Zhang, X., Korpelainen, H., and Li, C. (2012). Sex-related and stage-dependent
672 source-to-sink transition in populus cathayana grown at elevated co₂ and elevated
673 temperature. *Tree Physiology*, 32(11):1325–1338.

Supporting Information

674 S.1 Supporting Figures

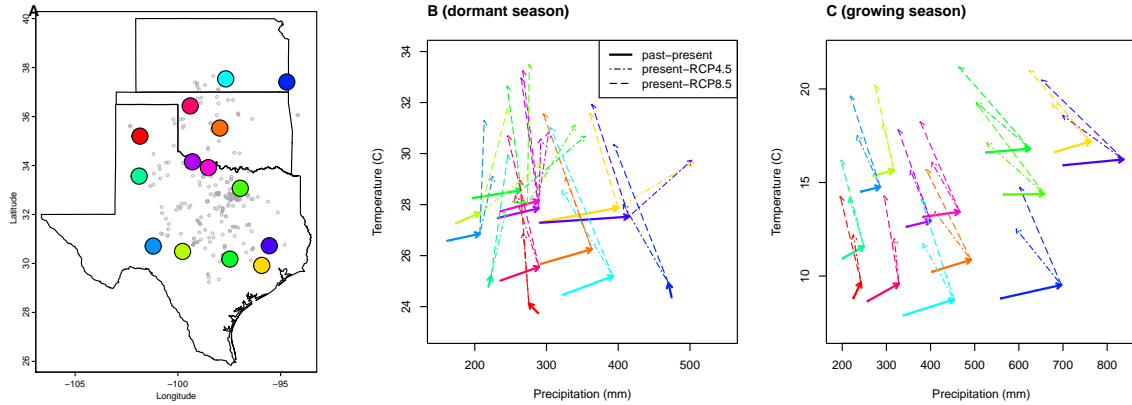


Figure S-1: (A), Common garden locations in Texas, Oklahoma, and Kansas (points) and (B,C) corresponding changes in growing and dormant season climate. Arrows in B,C connect past (1901-1930) and present (1990-2019) climate normals, and present and future (2071-2100) climate normals under RCP4.5 and RCP8.5 forecasts. Future forecasts are from MIROC5 but other climate models show similar patterns.

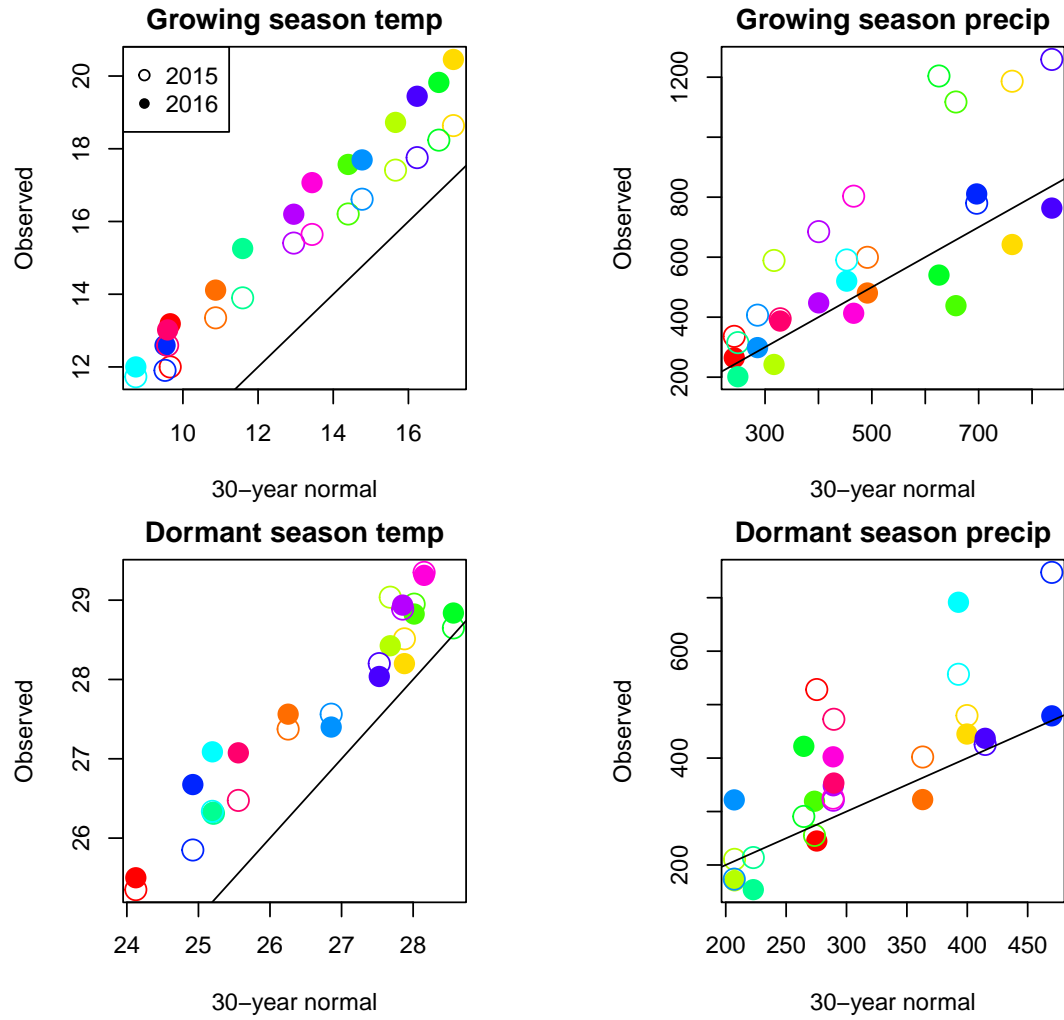


Figure S-2: Comparison of 30-year (1990-2019) climate normals and observed weather conditions at common garden sites during the 2014–15 and 2015–16 census periods. Temperature is in $^{\circ}\text{C}$ and precipitation is in mm . Colors represent sites and lines show the $y=x$ relationship.

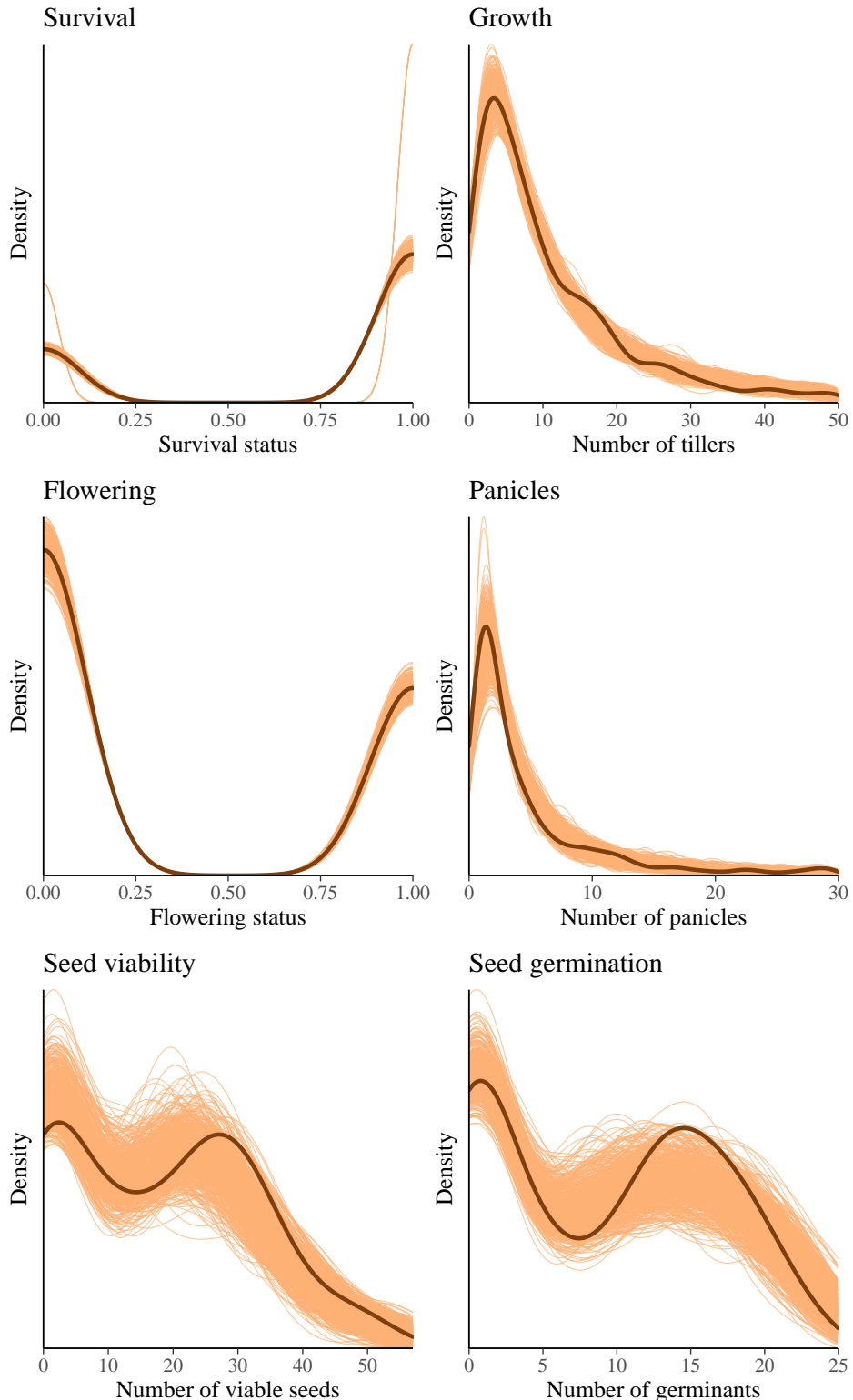


Figure S-3: Posterior predictive checks. Consistency between real data and simulated values suggests that the fitted vital rate models accurately describes the data. Graph shows density curves for the observed data (light orange) along with the simulated values (dark orange).

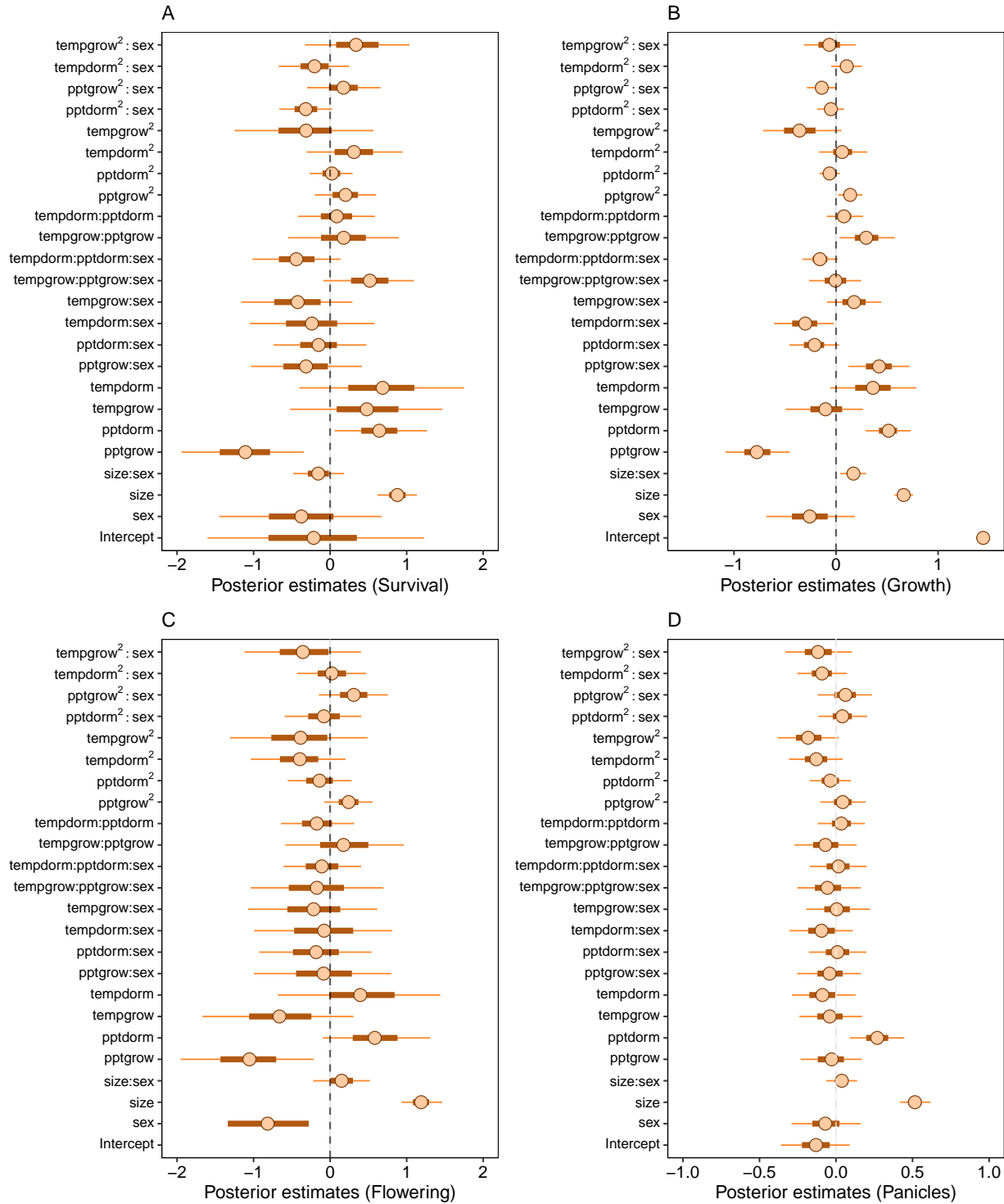


Figure S-4: Mean parameter values and 95% credible intervals of the posterior probability distributions. pptgrow is the precipitation of growing season, Tempgrow is the temperature of growing season, pptdorm is the temperature of dormant season, Tempdorm is the temperature of dormant season.

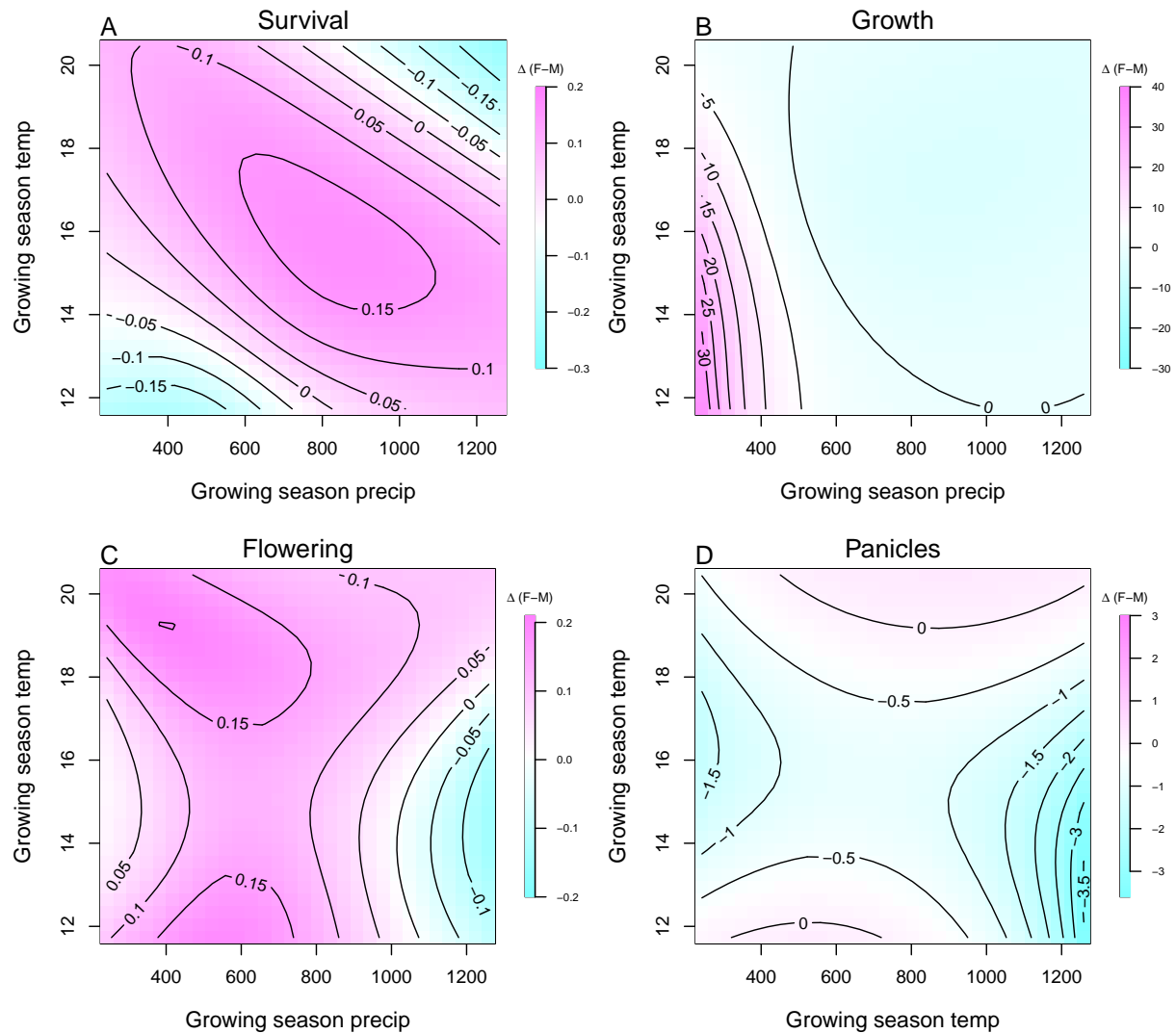


Figure S-5: Predicted difference in demographic response to climate across species range between female and male. Contours show predicted value of that difference conditional on precipitation and temperature of growing season

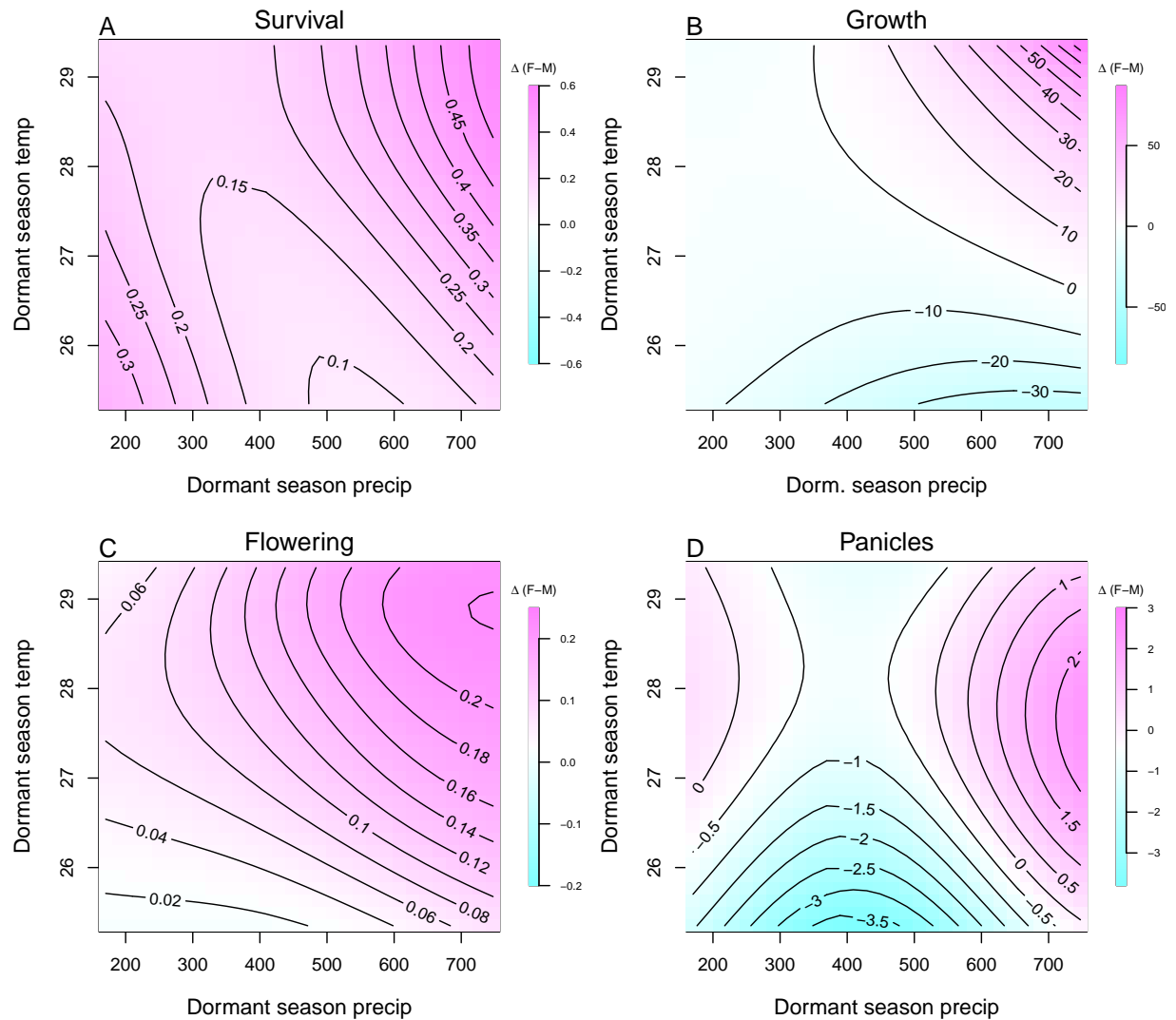


Figure S-6: Predicted difference in demographic response to climate across species range between female and male. Contours show predicted value of that difference conditional on precipitation and temperature of the dormant season

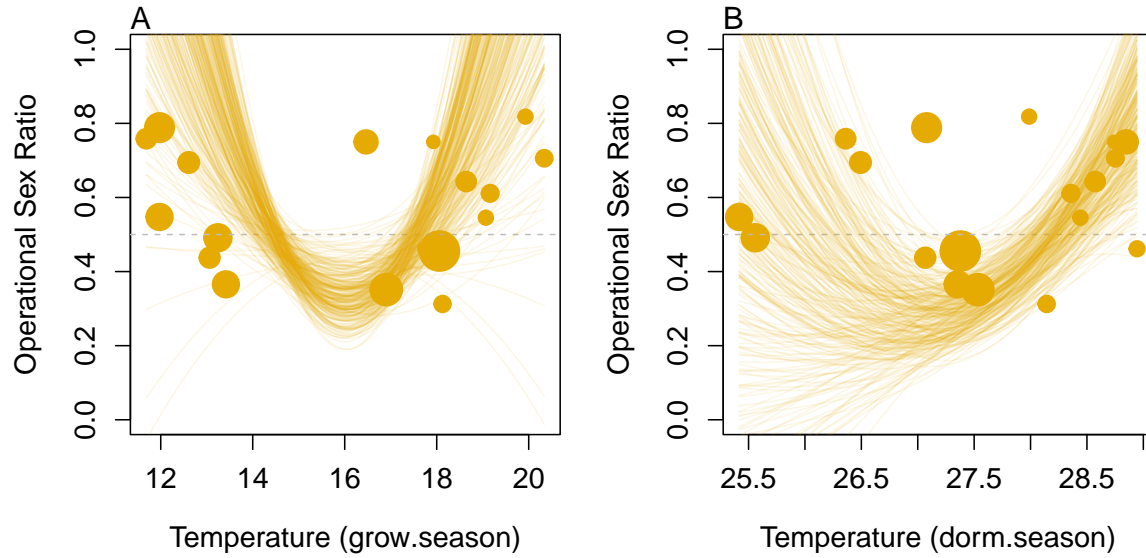


Figure S-7: Significant Operational Sex Ratio response across climate gradient. (A, B) Proportion of panicles that were females across temperature of the growing and dormant season

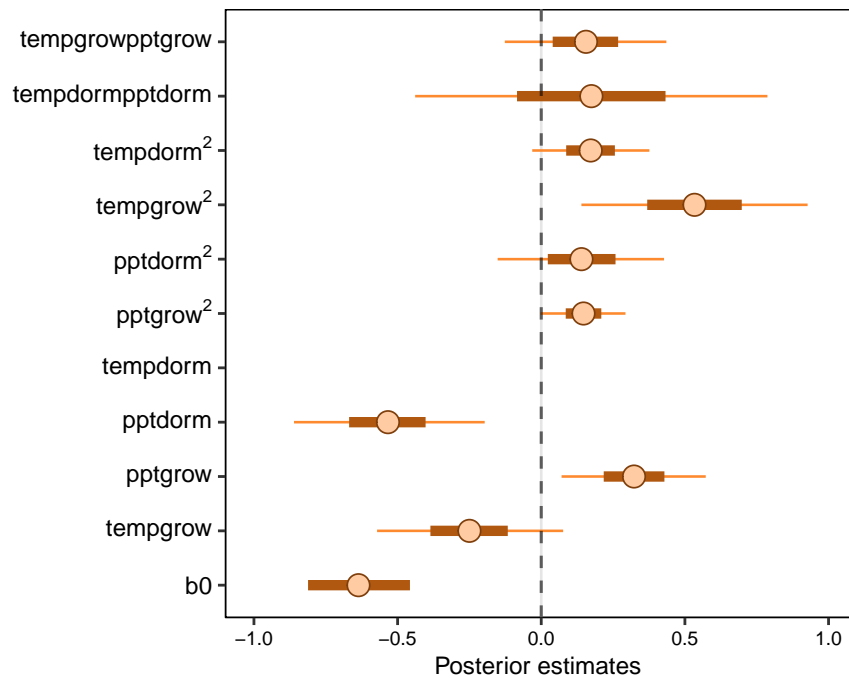


Figure S-8: Mean parameter values and 95% credible intervals of the posterior probability distributions for climate drivers of operational sex ratio (female fraction of total panicles) across common garden years and sites. pptgrow is the precipitation of growing season, Tempgrow is the temperature of growing season, pptdorm is the temperature of dormant season, Tempdorm is the temperature of dorm. season.

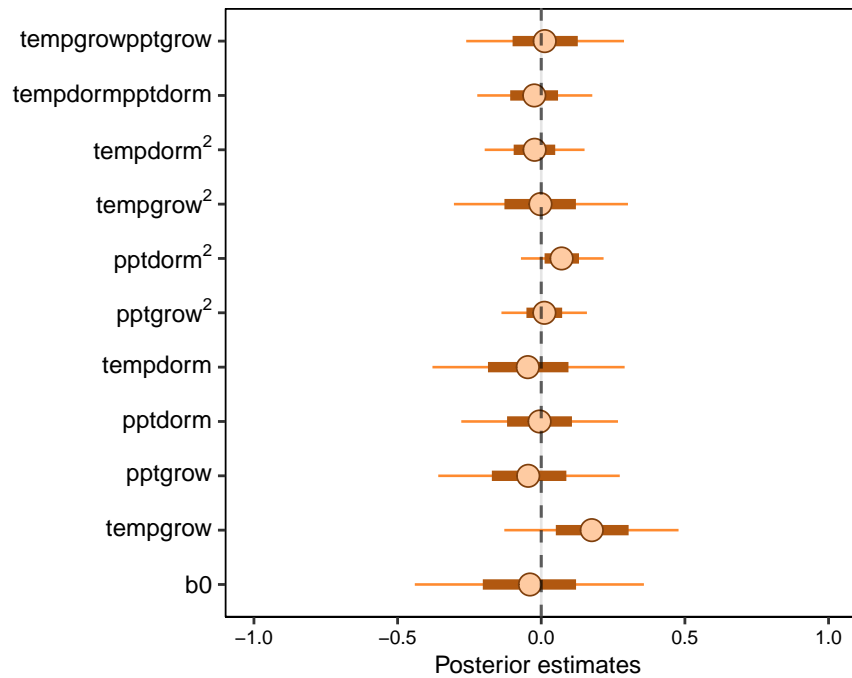


Figure S-9: Mean parameter values and 95% credible intervals of the posterior probability distributions for climate drivers of sex ratio (female fraction of the populations) across common garden years and sites. pptgrow is the precipitation of growing season, Tempgrow is the temperature of growing season, pptdorm is the temperature of dormant season, Tempdorm is the temperature of dormant season.

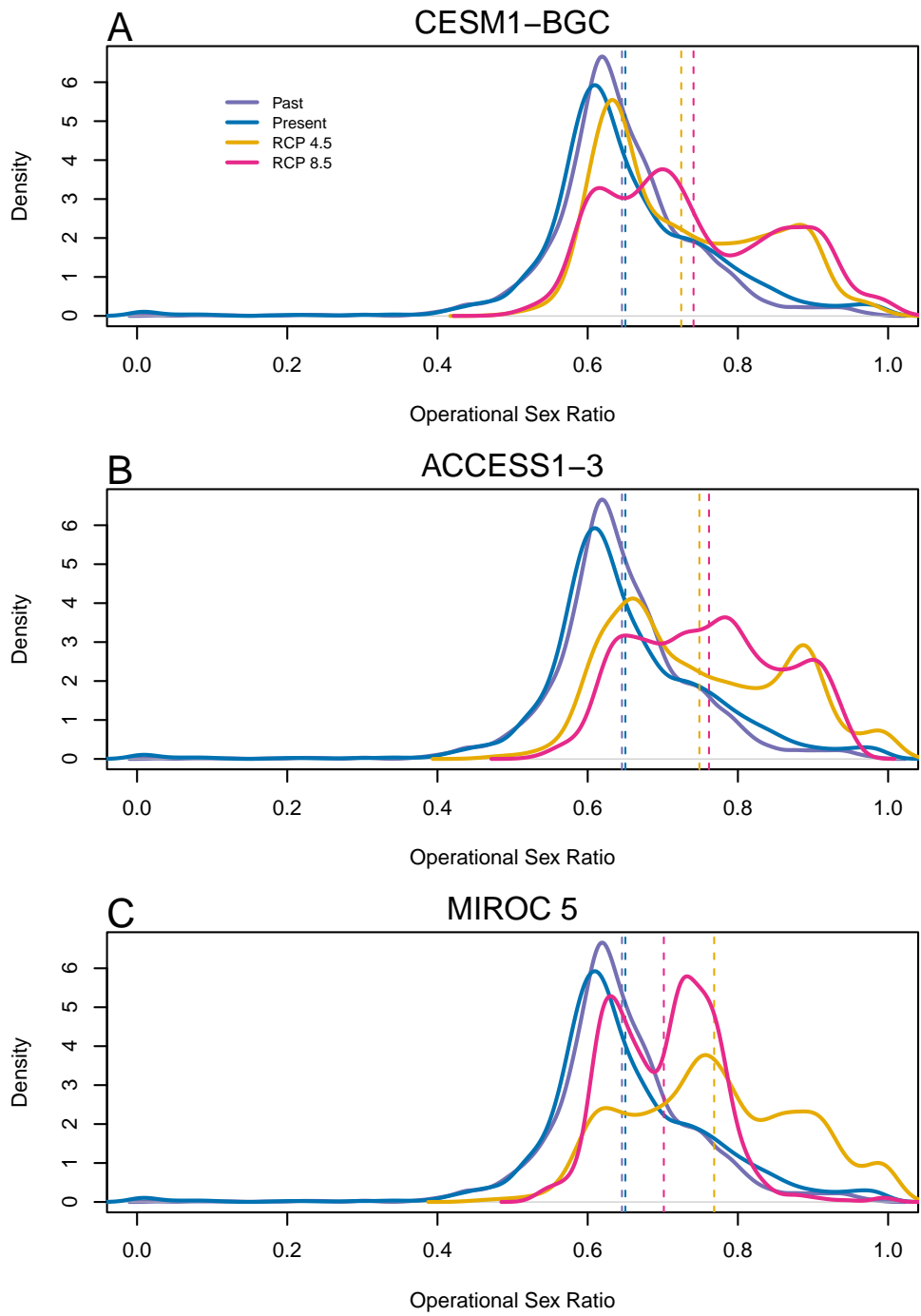


Figure S-10: Change in Operational Sex Ratio (proportion of female) over time (past, present, future). Future projections were based on A) MIROC 5, B) CES, C) ACC. The means for each model are shown as vertical dashed lines.

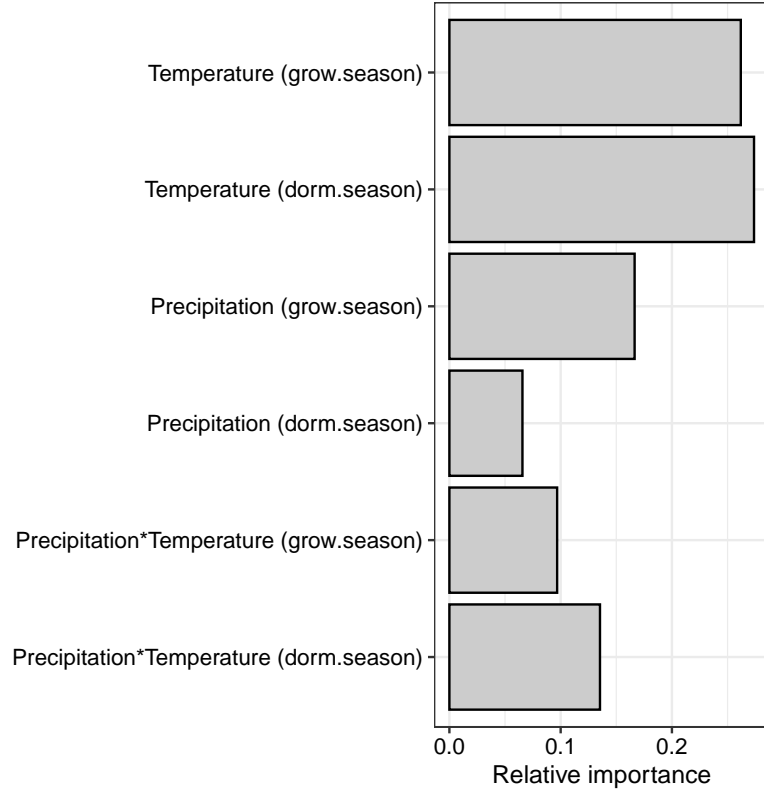


Figure S-11: Life Table Response Experiment: The bar represent the relative importance of each predictors.

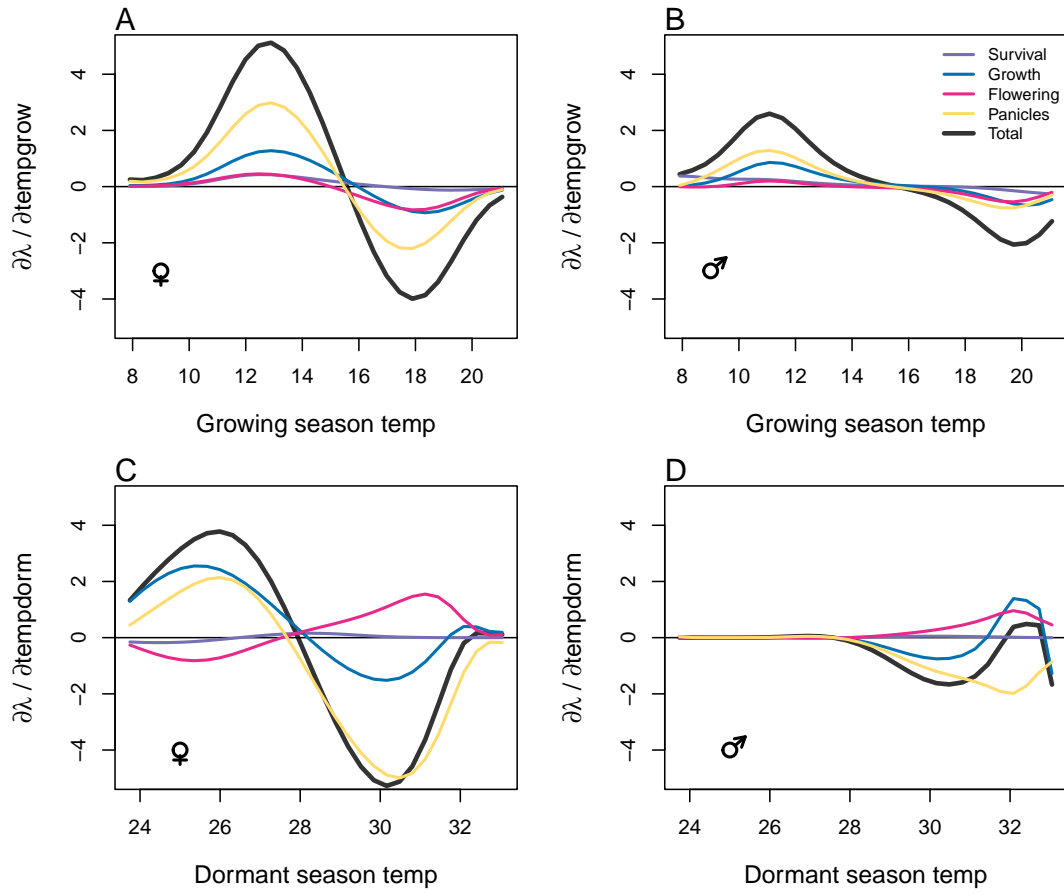


Figure S-12: Life table response experiment decomposition of the sensitivity of λ to seasonal climate into additive vital rate contributions of males and females based on posterior mean parameter estimates. (A) Temperature of growing season (contribution of female), (B) Temperature of growing season (contribution of male), (C) Temperature of dormant season (contribution of female) and (D) Temperature of dormant season (contribution of male).

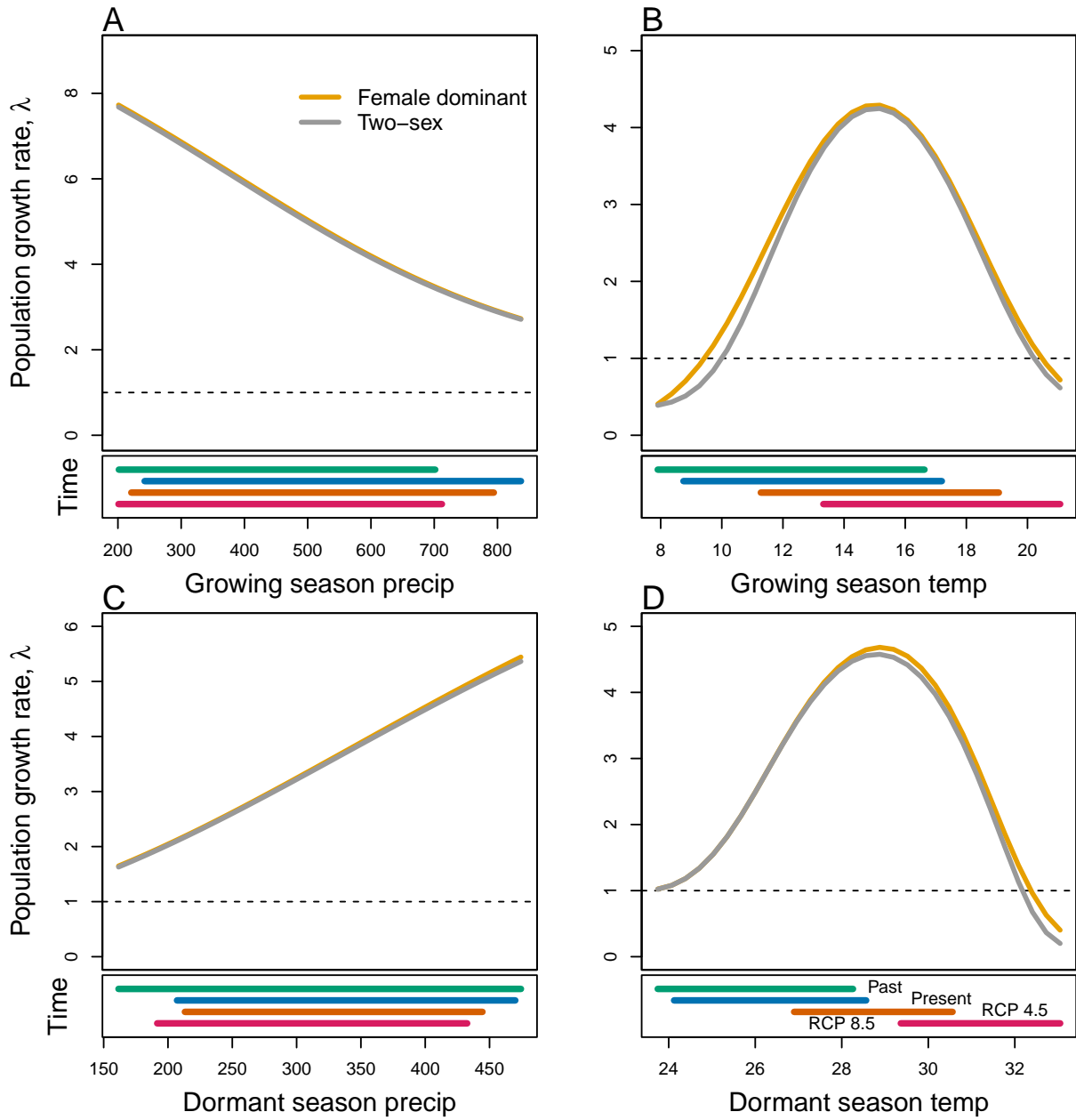


Figure S-13: Predicted population growth rate (λ) in different ranges of climate. (A) Precipitation of the growing season, (B) Temperature of the growing season, (C) Precipitation of the dormant season, (D) Temperature of the dormant season. The grey curve shows prediction by the two-sex matrix projection model that incorporates sex-specific demographic responses to climate with sex ratio dependent seed fertilization. The orange curve represents the prediction by the female dominant matrix projection model. The dashed horizontal line indicates the limit of population viability ($\lambda = 1$). Lower panels below each data panel show ranges of climate values for different time period (past climate, present and future climates). For future climate, we show a Representation Concentration Pathways (RCP) 4.5 and 8.5. Values population viability of (λ) are derived from the mean climate variables across 4 GCMs (MIROC5, ACCESS1-3, CESM1-BGC, CMCC-CM).

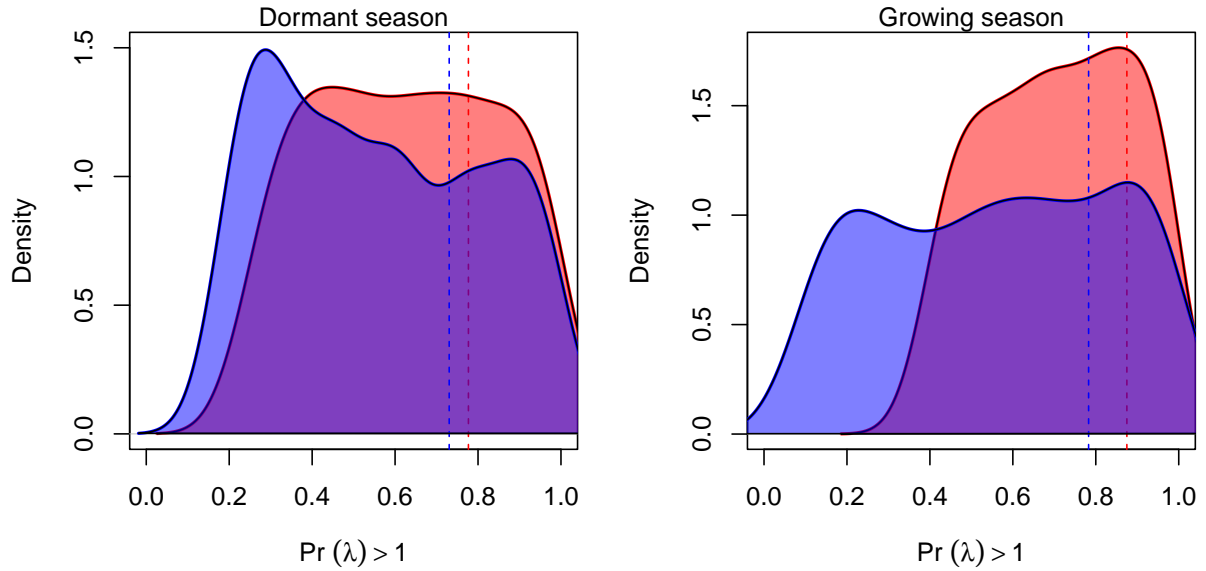


Figure S-14: Assessment of the statistical difference between the two-sex models and the female dominant model for the dormant and growing season. Plots show the density of $\text{Pr}(\lambda > 1)$ values for female dominant (pink) and two-sex models (violet) for each season. The means for each model are shown as vertical dashed lines.

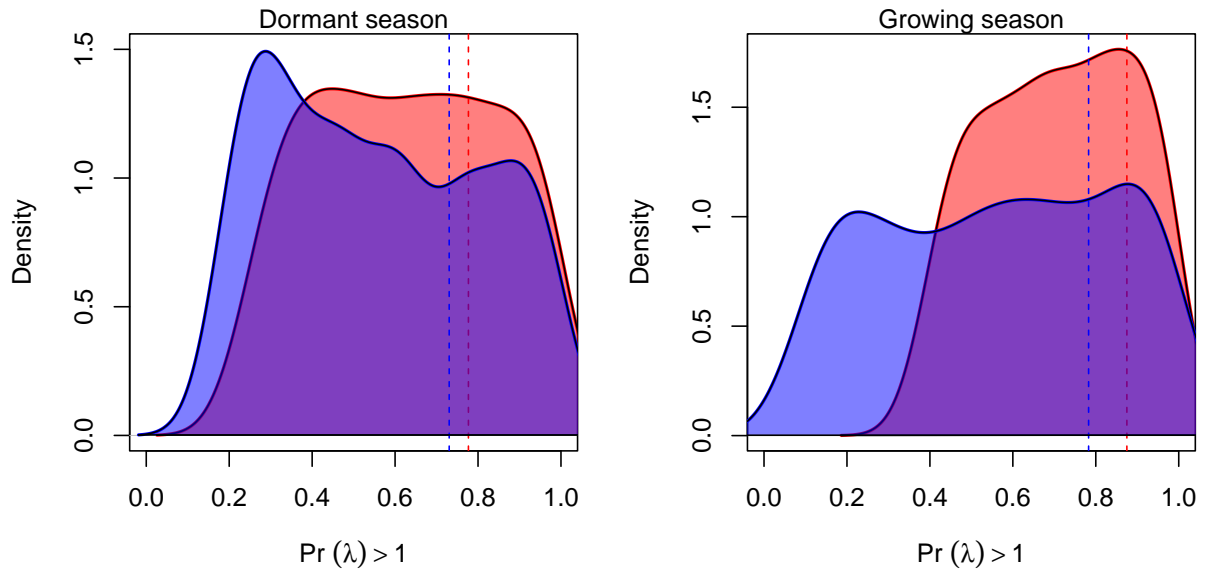


Figure S-15: Assessment of the statistical difference between the two-sex models and the female dominant model for the dormant and growing season. Plots show the density of $\text{Pr}(\lambda > 1)$ values for female dominant (pink) and two-sex models (violet) for each season. The means for each model are shown as vertical dashed lines.

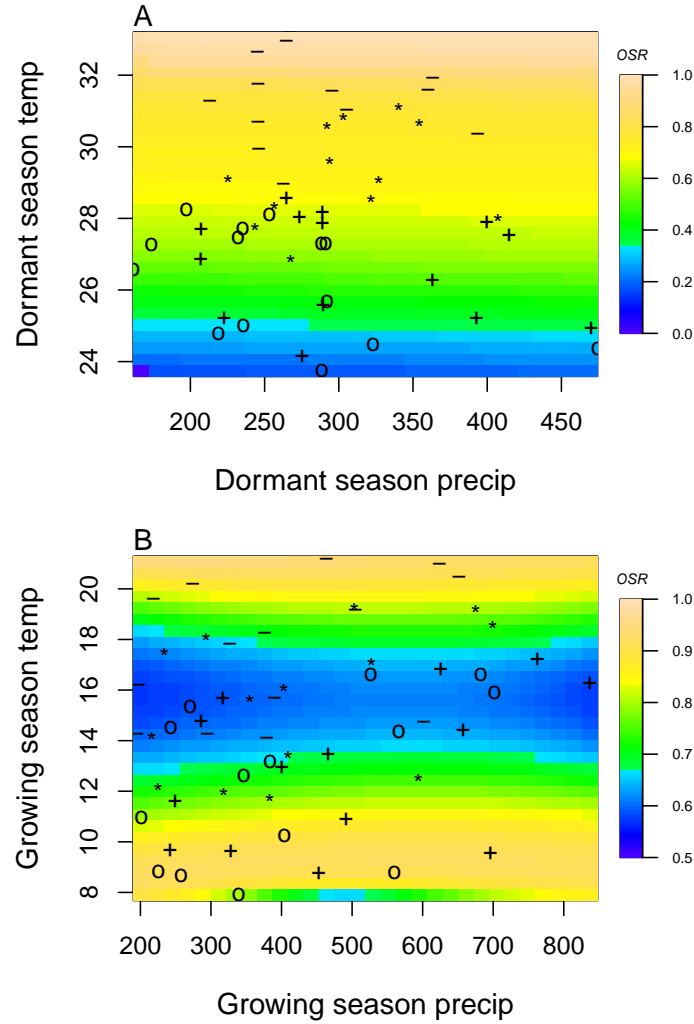


Figure S-16: A two-dimensional representation of the Operational Sex Ratio (OSR) over time (past, present and future climate conditions). OSR represents the proportion of females. Contours show predicted values of OSR conditional on precipitation and temperature of the dormant and growing season. Operational Sex Ratio during the dormant season for the two sex model (A), Operational Sex Ratio during the growing season for the two sex model (B). “**o**”: Past, “**+**”: Current, “*****”: RCP 4.5, “**-**”: RCP 8.5.

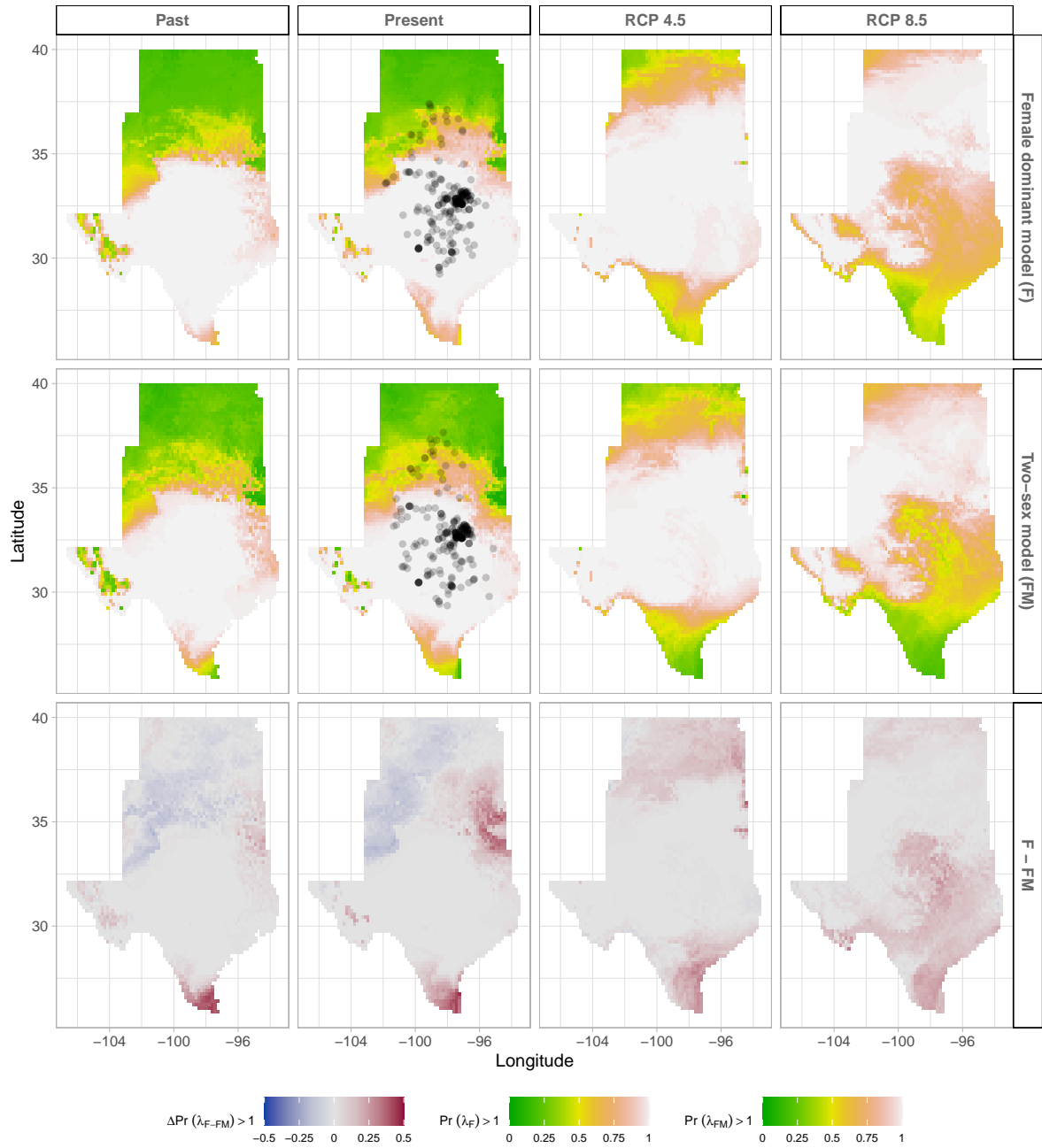


Figure S-17: Climate change favors range shift toward the North edge of the current range. (A) Past, (B) Current, (C and D) Future predicted range shift based on the predicted probabilities of self- sustaining populations, $\text{Pr}(\lambda > 1)$, using the two-sex model that incorporates sex- specific demographic responses to climate with sex ratio dependent seed fertilization. (E) Past, (F) Current, (G and H) Future predicted range shift based on the predicted probabilities of self- sustaining populations, $\text{Pr}(\lambda > 1)$, using the female dominant model. Future projections were based on the CESM1-BGC model. The black dots on panel B and F indicate all known presence points collected from GBIF from 1990 to 2019, which corresponds to the current condition in our prediction. The occurrences of GBIFs are distributed in with higher population fitness habitat $\text{Pr}(\lambda > 1)$, confirming that our study approach can reasonably predict range shifts.

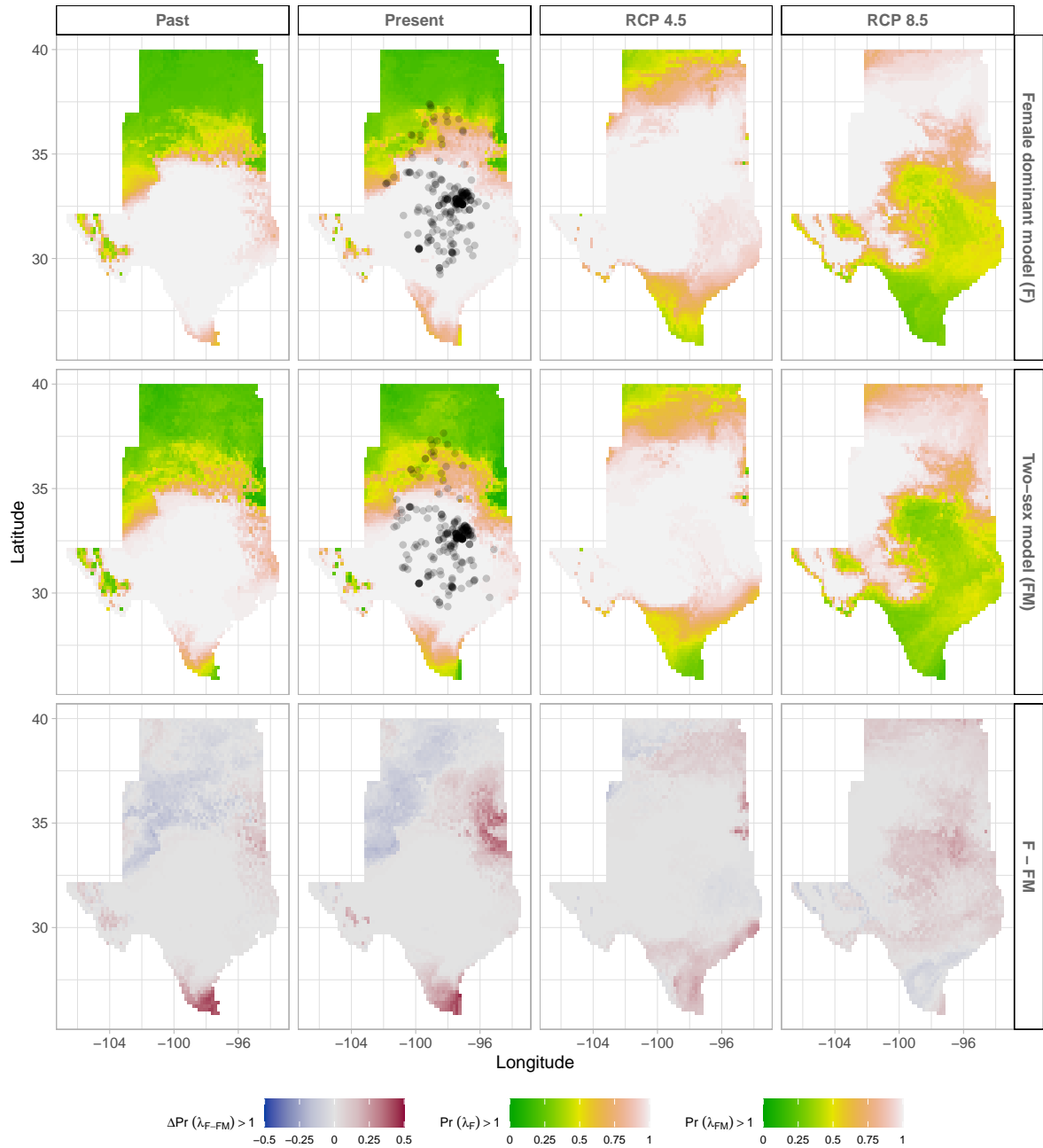


Figure S-18: Climate change favors range shift toward the North edge of the current range. (A) Past, (B) Current, (C and D) Future predicted range shift based on the predicted probabilities of self-sustaining populations, $\text{Pr}(\lambda > 1)$, using the two-sex model that incorporates sex-specific demographic responses to climate with sex ratio dependent seed fertilization. (E) Past, (F) Current, (G and H) Future predicted range shift based on the predicted probabilities of self-sustaining populations, $\text{Pr}(\lambda > 1)$, using the female dominant model. Future projections were based on the ACCESS model. The black dots on panel B and F indicate all known presence points collected from GBIF from 1990 to 2019, which corresponds to the current condition in our prediction. The occurrences of GBIFs are distributed in with higher population fitness habitat $\text{Pr}(\lambda > 1)$, confirming that our study approach can reasonably predict range shifts.

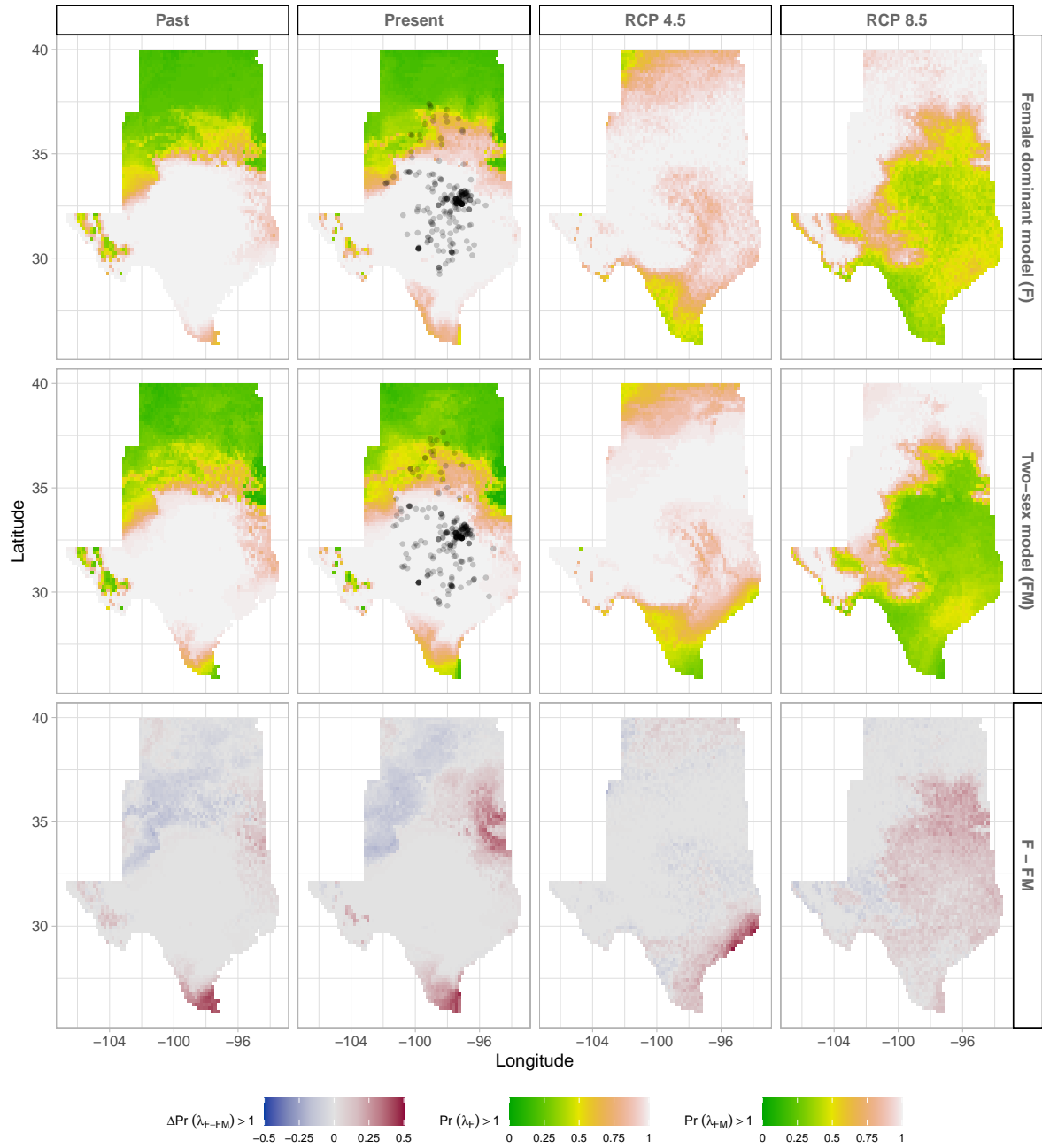


Figure S-19: Climate change favors range shift toward the North edge of the current range. (A) Past, (B) Current, (C and D) Future predicted range shift based on the predicted probabilities of self- sustaining populations, $\text{Pr}(\lambda > 1)$, using the two-sex model that incorporates sex- specific demographic responses to climate with sex ratio dependent seed fertilization. (E) Past, (F) Current, (G and H) Future predicted range shift based on the predicted probabilities of self- sustaining populations, $\text{Pr}(\lambda > 1)$, using the female dominant model. Future projections were based on the MIROC5 model. The black dots on panel B and F indicate all known presence points collected from GBIF from 1990 to 2019, which corresponds to the current condition in our prediction. The occurrences of GBIFs are distributed in with higher population fitness habitat $\text{Pr}(\lambda > 1)$, confirming that our study approach can reasonably predict range shifts.

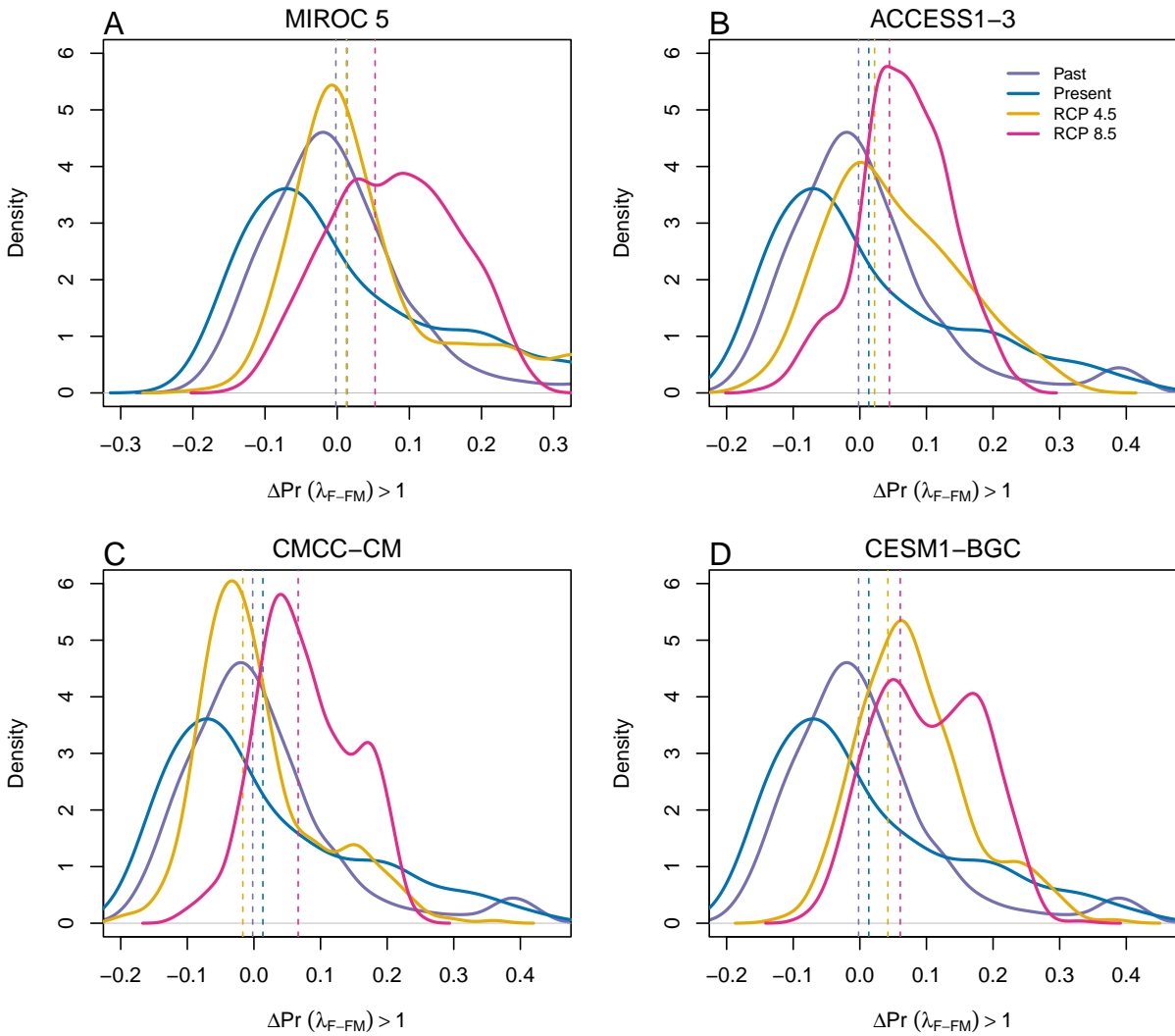


Figure S-20: Assessment of the statistical difference between the two-sex models and the female dominant model across and beyond species range for 4 GCMs. The means for each model are shown as vertical dashed lines.

675 **S.2 Supporting Methods**

676 **S.2.1 Sex-specific demographic responses to climatic variation across
677 common garden sites**

Vital rate models were fit with the same linear predictors for the expected value (μ)(Eq.S.1):

$$\begin{aligned}\mu = & \beta_0 + \beta_1 size + \beta_2 sex + \beta_3 pptgrow + \beta_4 pptdorm + \beta_5 tempgrow + \beta_6 tempdorm \\ & + \beta_7 pptgrow * sex + \beta_8 pptdorm * sex + \beta_9 tempgrow * sex + \beta_{10} tempdorm * sex \\ & + \beta_{11} size * sex + \beta_{12} pptgrow * tempgrow + \beta_{13} pptdorm * tempdorm \\ & + \beta_{14} pptgrow * tempgrow * sex + \beta_{15} pptdorm * tempdorm * sex + \beta_{16} pptgrow^2 \\ & + \beta_{17} pptdorm^2 + \beta_{18} tempgrow^2 + \beta_{19} tempdorm^2 + \beta_{20} pptgrow^2 * sex \\ & + \beta_{21} pptdorm^2 * sex + \beta_{22} tempgrow^2 * sex + \beta_{23} tempdorm^2 * sex + \phi + \rho + \nu\end{aligned}\quad (\text{S.1})$$

678 where β_0 is the grand mean intercept, β_1 is the size dependent slopes. *size* was on a natural
679 logarithm scale. $\beta_2 \dots \beta_{13}$ represent the climate dependent slopes. $\beta_{14} \dots \beta_{23}$ represent the
680 sex-climate interaction slopes. *pptgrow* is the precipitation of the growing season, *tempgrow*
681 is the temperature of the growing season, *pptdorm* is the precipitation of the dormant season,
682 *tempdorm* is the temperature of the dormant season.

683 **S.2.2 Sex ratio responses to climatic variation across common garden sites**

To understand the impact of climatic variation across common garden sites on sex ratio, OSR
and SR models using the same linear predictors for the expected value (ν)(Eq.S.2):

$$\begin{aligned}\nu = & \omega_0 + \omega_1 pptgrow + \omega_2 pptdorm + \omega_3 tempgrow + \omega_4 tempdorm + \\ & \omega_5 pptgrow^2 + \omega_6 pptdorm^2 + \omega_7 tempgrow^2 + \omega_8 tempdorm^2 + \epsilon\end{aligned}\quad (\text{S.2})$$

684 where *OSR* is the proportion of panicles that were female or proportion of female individuals
685 in the experimental populations, *c* is the climate. ω_0 is the intercept, $\omega_1, \dots, \omega_8$ are the climate
686 dependent slopes. ϵ is error term.

687 **S.2.3 Sex ratio experiment**

To estimate the probability of seed viability, the germination rate and the effect of sex-ratio
variation on female reproductive success, we conducted a sex-ratio experiment at one site
near the center of the range to estimate the effect of sex-ratio variation on female reproductive

success. The details of the experiment are provided in Compagnoni et al. (2017) and Miller and Compagnoni (2022b). Here we provide a summary of the experiment. We established 124 experimental populations in plots measuring 0.4 x 0.4m and separated by at least 15m from each other. We varied population density (1-48 plants/plot) and sex ratio (0%-100% female) across the experimental populations, and we replicated 34 combinations of density and sex ratio. We collected panicles from a subset of females in each plot and recorded the number of seeds in each panicle. We assessed reproductive success (seeds fertilized) using greenhouse-based germination and trazolium-based seed viability assays. Seed viability was modeled with a binomial distribution where the probability of viability (v) was given by:

$$v = v_0 * (1 - OSR^\alpha) \quad (\text{S.3})$$

688 where OSR is the proportion of panicles that were female in the experimental populations.
 689 α is the parameter that control for how viability declines with increasing female bias. Further,
 690 germination rate was modeled using a binomial distribution to model the germination
 691 data from greenhouse trials. Given that germination was conditional on seed viability, the
 692 probability of success was given by the product $v * g$, where v is a function of OSR (Eq. S.3)
 693 and g is assumed to be constant.